Coupled-mode theory for light propagation through deep nonlinear gratings

C. Martijn de Sterke and David G. Salinas*
School of Physics and Optical Fibre Technology Centre, University of Sydney, 2006, Australia

J. E. Sipe
Department of Physics, University of Toronto, Toronto, Ontario, Canada M5S 1A7

(Received 16 January 1996)

In ordinary coupled-mode theory, the standard tool to analyze optical grating structures in both linear and nonlinear regimes, the grating is usually assumed to be shallow. Here we generalize this theory in a systematic way to include deep gratings. We do so by expanding in the exact eigenfunctions of the linear structure (the Bloch functions) rather than simply in the forward and backward propagating modes. We show that the resulting equations for deep gratings are qualitatively similar to those for shallow ones, except that the value of some of the coefficients is different and that some additional nonlinear terms arise. We also discuss solutions to these equations and point out differences from solutions of the conventional theory. [S1063-651X(96)06208-3]

PACS number(s): 42.79.Dj

I. INTRODUCTION

Though periodic structures have been studied for many years, recent advances in grating fabrication in optical fibers have renewed the interest in this area. In the structures considered here, the light propagates through the grating in a direction perpendicular to the rulings. While most applications of fiber gratings, such as filters and dispersion compensators, make use of the *linear* properties of Bragg gratings, theoretical work on the nonlinear properties of these structures (see, e.g. [1–8]), as well as initial experiments [9–13], has resulted in significant insights.

The experiments by Eggleton *et al.* [13] most closely match the theory described in this paper. In these experiments short intense pulses from a Nd:YLF laser are incident on a grating written in the core of an optical fiber, while the light transmitted by the grating is monitored. Among the observations in these experiments is that of pulse narrowing upon propagation through the grating. This is explained in terms of the formation of grating solitons: pulses that can propagate through the grating structure undistorted by balancing the dispersion introduced by the grating with the nonlinearity.

While periodic structures are, of course, three dimensional, it is often possible to avoid explicit reference to the dimensions perpendicular to the direction of propagation. Typically, the argument leading to this approximation refers to the transverse modes of the structure (for example, the bound modes of an optical fiber) and assumes that the modal profiles are essentially unaffected by the periodicity; under this assumption the problem becomes one dimensional [14,15]. Though it is straightforward to calculate the optical properties of a one-dimensional periodic structure exactly by integrating the Maxwell equations [16], it is often advantageous to use a coupled-mode formalism, in which one works with slowly varying electric-field envelope functions rather than with the electric and magnetic fields themselves; such approaches are numerically more efficient and can give more physical insight. The coupled-mode equations are usually derived heuristically, assuming the grating to be *shallow*, forming a weak modulation superimposed on a uniform background [17]. This assumption allows one to expand the electric field simply in terms of the so-called forward and backward propagating modes of the uniform structure, each with a slowly varying amplitude induced by the grating.

For deep gratings, i.e., gratings for which the modulation depth of the grating is a substantial fraction of the average refractive index, the approach sketched in the paragraph above can no longer be applied so easily. There are two reasons for this. The first of these is that if the grating is deep, then it is possible that the mode profiles of the structure are significantly affected by it; this would lead to a breakdown of the one-dimensional treatment. However, sufficiently far from cutoff modal profiles often do not change much, even if the refractive indices change considerably. The second reason is more fundamental: if the grating is deep then a standard coupled-mode approach applied naively would lead to envelope functions that are not slowly varying, invalidating the assumptions. This is clearly an indication that the forward and backward propagating modes of the uniform structure are no longer appropriate expansion functions.

Conventional coupled-mode theory can be applied to almost all fiber gratings, including those used in the experiments of Eggleton *et al.*, where the refractive index modulation is of order 10^{-4}. However, it should be noted that in fiber geometries refractive index changes as large as 0.04 have been reported [18]. With such changes the validity of the shallow grating assumption is no longer guaranteed. More markedly, in periodic semiconductor structures containing, say, GaAs and AlAs, with refractive indices 3.59 and 2.98, respectively, the shallow grating assumption is clearly suspicious, while in proposed semiconductor-polymer systems, with refractive index ratios of over 2, conventional

*Present address: Department of Physics, Cornell University, Ithaca, NY 14853.

coupled-mode theory must fail. We also note that in the derivation of conventional coupled-mode theory only the average value of the nonlinearity over a period is included; any spatial variations of the nonlinearity on the scale of a single period is neglected. Conventional coupled-mode theory is thus not expected to be applicable to gratings in which one of the constituents is, say, much more nonlinear than the other. In this paper we use the phrase ''deep grating'' to refer to gratings where the linear index of refraction varies over a significant fraction of its average value, as well as to shallow nonlinear gratings where the nonlinearity varies over the scale of a single period. We show below that these effects have comparable consequences on the description of the propagation of light through the grating structure.

As sketched above, for deep gratings one can identify two different problems in identifying coupled-mode theory. In this paper we assume from the outset that the transverse dimensions have been properly integrated out; in effect, therefore, we model the periodic structure as a thin-film stack. We address the second, more fundamental point listed above, namely, that the forward and backward propagating modes of the uniform medium are inappropriate expansion functions for the electromagnetic field. One might expect that in such a case one would have to revert to the full Maxwell equations. While this is of course possible, we show here that, somewhat surprisingly, in certain regimes it is possible to describe deep gratings with a set of coupled-mode equations very similar to the well-known coupled-mode equations for shallow gratings. Thus a whole body of formalism and insights can be carried over directly to problems involving deep gratings. The key to constructing such a generalization is to rely on the Bloch functions of the linear periodic medium [19–21] to identify the appropriate expansion functions. Since the Bloch functions are a property of the linear structure, they can, in principle, be found straightforwardly, for example, using methods developed in solid state physics [19]. We show that if the theory for deep gratings is based on the Bloch functions, the resulting equations for the field envelopes are very similar to those for shallow gratings, except for different values for some of the coefficients and some different nonlinear terms. Of equal importance perhaps is that we present a systematic approach to solving this class of problems.

One of our main conclusions is that the grating solitons observed by Eggleton *et al.* [13] are not peculiar to shallow gratings; indeed, though they are affected in some details, the concept appears to be generic to nonlinear periodic media. Though grating solitons in deep gratings were studied before in limiting cases [2,3], the present work is much more general.

The outline of this paper is as follows. In Sec. II we discuss the linear properties of one-dimensional periodic media. Then, in Sec. III we derive the $\mathbf{k}\cdot\mathbf{V}$ expansion, the optical equivalent of the $\mathbf{k}\cdot\mathbf{p}$ expansion in solid state physics [19]. In Sec. IV we introduce the multiple-scales method, which we then apply in Secs. V and VI to nonlinear periodic media. Then, in Sec. VII we transform the resulting equations to the standard form, leading to the coupled-mode equations for deep gratings. We also discuss some of the features of these equations. In Sec. VIII we give the values of the coefficients in the present coupled-mode equations. Then, in Sec. IX we present some of the solutions to these equations. Finally, we discuss our results in Sec. X.

II. LINEAR EQUATIONS AND BASIS FUNCTIONS

As discussed in Sec. I, we idealize our fields as depending on only a single spatial variable, say, z; this reduces the problem to a one-dimensional analysis. We then write for the electric and magnetic fields, respectively,

$$\mathbf{E}(\mathbf{r},t)=\hat{\mathbf{x}}E(z,t),$$
$$\mathbf{H}(\mathbf{r},t)=\hat{\mathbf{y}}H(z,t). \tag{1}$$

We neglect any magnetic effects, assume that any frequency dependence of the dielectric constant $\epsilon(z)$ may be neglected, and ignore for the moment any nonlinearity in the optical response. The Maxwell equations then simplify to

$$\frac{\partial H}{\partial t}=-\frac{1}{\mu_0}\frac{\partial E}{\partial z},$$
$$\frac{\partial E}{\partial t}=-\frac{1}{\epsilon_0 n^2(z)}\frac{\partial H}{\partial z}, \tag{2}$$

where μ_0 and ϵ_0 are the permeability and permittivity of free space, respectively. We have introduced the spatially varying index of refraction $n(z)=[\epsilon(z)/\epsilon_0]^{1/2}$, which we take here to be purely real, neglecting any extinction due to absorption or scattering. In applications dealing with a guiding structure, $n(z)$ should be taken as the effective index of refraction [14].

Instead of working with the fields $E(z,t)$ and $H(z,t)$, it is more convenient to introduce local mode amplitudes $A^{\pm}(z,t)$ [17,21]. Recall that, if $n(z)$ were uniform, a wave traveling towards $z=+\infty$ would have magnetic and electric fields related by $H=(nE)/Z_0$, where $Z_0=(\mu_0/\epsilon_0)^{1/2}$ is the vacuum impedance; similarly, a wave traveling toward $z=-\infty$ would have $H=-(nE)/Z_0$. This leads us to introduce

$$A^{\pm}(z,t)=\frac{1}{2}\left[\frac{n(z)}{n_0}\right]^{1/2}\left[E(z,t)\pm Z_0\frac{H(z,t)}{n(z)}\right], \tag{3}$$

where n_0 is a reference refractive index. In definition (3) we would expect $A^{+}(z,t)$ to identify the local component of the electromagnetic field propagating in the forward direction and $A^{-}(z,t)$ that propagating in the backward direction. The usefulness of these amplitudes, and the motivation for the precise form of the definitions (3), has been discussed earlier [17]. From Eq. (2) we can immediately derive the equations the $A^{\pm}$ must satisfy

$$\frac{\partial A^{\pm}(z,t)}{\partial z}\pm\frac{n(z)}{c}\frac{\partial A^{\pm}(z,t)}{\partial t}=\frac{1}{2}\left[\frac{\partial[\ln n(z)]}{\partial z}\right]A^{\mp}(z,t), \tag{4}$$

where the speed of light $c=(\mu_0\epsilon_0)^{-1/2}$ or

$$in(z)\frac{\partial\mathbf{A}}{\partial t}=\mathbf{M}\cdot\mathbf{A}, \tag{5}$$

where we have introduced the column vector

$$\mathbf{A}\equiv\begin{bmatrix}A^{+}(z,t)\\A^{-}(z,t)\end{bmatrix} \tag{6}$$

and the matrix differential operator

$$\mathbf{M}\equiv\begin{bmatrix}-ic\dfrac{\partial}{\partial z} & \dfrac{1}{2}ic\left(\dfrac{\partial[\ln n(z)]}{\partial z}\right)\\ -\dfrac{1}{2}ic\left(\dfrac{\partial[\ln n(z)]}{\partial z}\right) & ic\dfrac{\partial}{\partial z}\end{bmatrix}. \tag{7}$$

In the notation for column vectors and matrix operators, such as $\mathbf{A}$ and $\mathbf{M}$, respectively, we leave implicit the dependence on z (and $\partial/\partial z$).

As the form of Eq. (5) suggests, the eigenvectors of the matrix $n^{-1}(z)\mathbf{M}$ form a useful expansion basis. Writing the eigenvectors as $\mathbf{\Psi}_\mu$,

$$\mathbf{\Psi}_\mu\equiv\begin{bmatrix}\psi_\mu^{+}(z)\\ \psi_\mu^{-}(z)\end{bmatrix}, \tag{8}$$

and the eigenvalues as ω_μ, it is convenient to write the eigenvalue equation in the form

$$\mathbf{M}\cdot\mathbf{\Psi}_\mu=\omega_\mu\mathbf{n}\cdot\mathbf{\Psi}_\mu, \tag{9}$$

where

$$\mathbf{n}\equiv\begin{bmatrix}n(z) & 0\\ 0 & n(z)\end{bmatrix}. \tag{10}$$

It is easy to confirm that the operator $\mathbf{M}$ is Hermitian: $(\mathbf{\Psi}_\nu^{\dagger}\cdot\mathbf{M}\cdot\mathbf{\Psi}_\mu)=(\mathbf{\Psi}_\mu^{\dagger}\cdot\mathbf{M}\cdot\mathbf{\Psi}_\nu)^*$, where the row vector

$$\mathbf{\Psi}_\mu^{\dagger}=[[\psi_\mu^{+}(z)]^*,[\psi_\mu^{-}(z)]^*] \tag{11}$$

and

$$(\mathbf{\Psi}_\nu^{\dagger}\cdot\mathbf{M}\cdot\mathbf{\Psi}_\mu)\equiv\int_0^L dz\,\mathbf{\Psi}_\nu^{\dagger}\cdot\mathbf{M}\cdot\mathbf{\Psi}_\mu. \tag{12}$$

Here L is a normalization length over which we apply periodic boundary conditions and thus the length over which we require the eigenfunctions $\mathbf{\Psi}_\mu$ to be periodic. From this it follows that the eigenvalues ω_μ are real and that eigenvectors of different eigenvalues are orthogonal through the metric $\mathbf{n}$,

$$(\mathbf{\Psi}_\nu^{\dagger}\cdot\mathbf{n}\cdot\mathbf{\Psi}_\mu)=0,\quad \omega_\mu\neq\omega_\nu. \tag{13}$$

Further, note that if $\mathbf{\Psi}_\mu$ satisfies Eq. (9) with eigenvalue ω_μ, then $\mathbf{\Psi}_\mu^*$ defined through

$$\mathbf{\Psi}_\mu^*\equiv\begin{bmatrix}[\psi_\mu^{+}(z)]^*\\ [\psi_\mu^{-}(z)]^*\end{bmatrix}, \tag{14}$$

satisfies that same equation with eigenvalue $-\omega_\mu$. Henceforth we restrict ourselves to positive ω_μ; then, since $\mathbf{A}$ must be real, it is convenient to expand solutions of Eq. (5) in the form

$$\mathbf{A}=\sum_\mu\,(f_\mu\mathbf{\Psi}_\mu e^{-i\omega_\mu t}+f_\mu^*\mathbf{\Psi}_\mu^* e^{i\omega_\mu t}), \tag{15}$$

where the constants f_μ are expansion coefficients.

Periodic structures

Our interest is in periodic media with a period that we take to be d, so that $n(z+d)=n(z)$; $L/d\equiv N$ is thus the number of unit cells in our normalization length. Before proceeding, it will be useful to relate our $\mathbf{\Psi}_\mu$ to the more common expansion functions used in such a problem, the Bloch functions for the electric field [20]. Recall first how these are introduced. Taking the z derivative of the first of Eqs. (2) and the t derivative of the second, we combine the results to obtain a second-order equation for $E(z,t)$ alone,

$$-c^2\frac{\partial^2}{\partial z^2}E(z,t)+n^2(z)\frac{\partial^2}{\partial t^2}E(z,t)=0. \tag{16}$$

Seeking then a solution of the form

$$E(z,t)=\phi_\mu(z)e^{-i\omega_\mu t}+\phi_\mu^*(z)e^{i\omega_\mu t}, \tag{17}$$

where the ω_μ is taken to be positive, we find that the $\phi_\mu(z)$ must satisfy

$$-c^2\frac{\partial^2\phi_\mu(z)}{\partial z^2}=\omega_\mu^2 n^2(z)\phi_\mu(z). \tag{18}$$

From Bloch's theorem [19] the Bloch functions $\phi_\mu(z)$ can be chosen to be of the form

$$\phi_{mk}(z)=e^{ikz}u_{mk}(z). \tag{19}$$

Here the general index μ has been replaced by a band index m and a reduced wave number k [19]; k must be of the form $2\pi p/L$, where p is an integer, to guarantee periodicity over the normalization length L and $u_{mk}(z+d)=u_{mk}(z)$. A typical dispersion relation for the ω_{mk} is sketched in Fig. 1; we take the values of k to be in the first Brillouin zone, i.e., in the range $-\pi/d<k\leq\pi/d$. From Eq. (18) it is clear that eigenfunctions $\phi_{km}(z)$ of different eigenvalues are orthogonal through the metric $n^2(z)$; thus we can write [3]

$$\int_0^L\phi_{m'k'}^*(z)n^2(z)\phi_{mk}(z)dz=N\delta_{m'm}\delta_{k'k}, \tag{20}$$

where we have chosen the normalization constant $N=L/d$ to facilitate the passage to the $L\to\infty$ limit.

Once a solution (17) for $E(z,t)$ is identified, the corresponding $H(z,t)$ can be found from the first of Eqs. (2); the corresponding $A^{\pm}(z,t)$ then follow immediately from Eq. (3). Referring then to Eq. (15), we can immediately identify the $\psi_{mk}^{\pm}(z)$ associated with each $\phi_{mk}(z)$; we find

$$\psi_{mk}^{\pm}(z)=\frac{1}{2}\left[\sqrt{n(z)}\phi_{mk}(z)\mp\frac{ic}{\omega_{mk}}\frac{1}{\sqrt{n(z)}}\frac{\partial\phi_{mk}(z)}{\partial z}\right], \tag{21}$$

where the overall factor on the right-hand side is chosen to ensure that

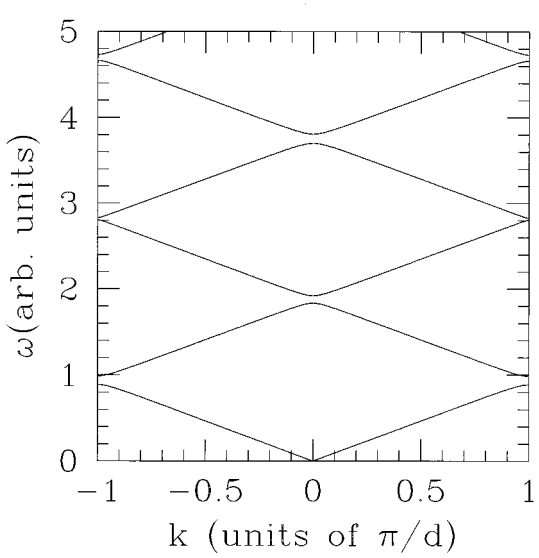

FIG. 1. Typical example of a one-dimensional photonic band structure, showing (angular) frequency as a function of k (in units of π). The frequency gaps correspond to regions of high reflection.

$$(\boldsymbol{\Psi}^{\dagger}_{m'k'}\cdot\mathbf{n}\cdot\boldsymbol{\Psi}_{mk})=N\delta_{m'm}\delta_{k'k}. \tag{22}$$

When a solution or approximation for the $\phi_{mk}(z)$ is constructed, the corresponding $\boldsymbol{\Psi}_{mk}$ then follow immediately from Eq. (21); thus, we will often refer loosely to the $\boldsymbol{\Psi}_{mk}$ as ''Bloch functions.'' We shall see in Sec. IV that, within a multiple-scales analysis, the inclusion of nonlinearity is easier using the $\boldsymbol{\Psi}_{mk}$ as a basis than using the ϕ_{mk}. This can be traced back to the fact that an expansion corresponding to the $\mathbf{k}\cdot\mathbf{p}$ expansion used in describing an electron in a periodic potential is simpler, and more similar in form to the electronic result, with the use of the $\boldsymbol{\Psi}_{mk}$ as a basis instead of the ϕ_{mk} [22]. This, in turn, occurs because Eq. (5), with its single time derivative, is closer in form to the Schrödinger equation than is Eq. (16). It is to the above-mentioned expansion that we turn in the next section.

III. THE k·V EXPANSION

Associated with each k (see Fig. 1) is a set of $\boldsymbol{\Psi}_{mk}$, one for each of the band indices m. In this section we seek expressions for $\omega'_{mk}\equiv\partial\omega_{mk}/\partial k$ and $\omega''_{mk}\equiv\partial^2\omega_{mk}/\partial k^2$ in terms of (all of the) $\boldsymbol{\Psi}_{qk}$ at only the k of interest; such expressions appear naturally in the development of the following sections and it will be useful to be able to identify them as the group velocity ω'_{mk} and the group velocity dispersion ω''_{mk}.

We begin by noting that we may write the $\psi^{\pm}_{mk}$ of Eq. (21) as

$$\psi^{\pm}_{mk}(z)=\frac{1}{2}\left[\sqrt{n(z)}u_{mk}(z)\pm\frac{ck}{\omega_{mk}}\frac{u_{mk}(z)}{\sqrt{n(z)}}\mp\frac{ic}{\omega_{mk}}\frac{1}{\sqrt{n(z)}}\frac{\partial u_{mk}(z)}{\partial z}\right]e^{ikz}\equiv h^{\pm}_{mk}(z)e^{ikz}, \tag{23}$$

where we have used Eq. (19) for the ϕ_{mk}; note that from the periodicity of the $u_{mk}(z)$ we find that we also have $h^{\pm}_{mk}(z+d)=h^{\pm}_{mk}(z)$. Defining a column vector $\mathbf{h}_{mk}$ in the obvious way, we have

$$\boldsymbol{\Psi}_{mk}=\mathbf{h}_{mk}e^{ikz} \tag{24}$$

and we find

$$\mathbf{M}\cdot(\mathbf{h}_{mk}e^{ikz})=e^{ikz}(\mathbf{M}+k\mathbf{V})\cdot\mathbf{h}_{mk}, \tag{25}$$

where

$$\mathbf{V}\equiv\begin{bmatrix}c & 0\\ 0 & -c\end{bmatrix}. \tag{26}$$

The expression in Eq. (25) also equals $\omega_{mk}\mathbf{n}\cdot\boldsymbol{\Psi}_{mk}$ [Eq. (9)], so using Eq. (24) we find

$$(\mathbf{M}+k\mathbf{V})\cdot\mathbf{h}_{mk}=\omega_{mk}\mathbf{n}\cdot\mathbf{h}_{mk}. \tag{27}$$

Since we want to expand the photonic bands about a particular crystal momentum (indicated by K) [19], we set $k=K+\delta k$ and define $\mathbf{H}_0\equiv\mathbf{M}+K\mathbf{V}$; Eq. (27) becomes

$$[\mathbf{H}_0+(\delta k)\mathbf{V}]\cdot\mathbf{h}_{mk}=\omega_{mk}\mathbf{n}\cdot\mathbf{h}_{mk}. \tag{28}$$

For k close to K we now seek an expansion in powers of the small parameter δk of $\mathbf{h}_{mk}$ and ω_{mk} about $\mathbf{h}_{mK}$ and ω_{mK}, respectively,

$$\omega_{mk}=\omega_{mK}+(\delta k)\omega^{(1)}_{mK}+(\delta k)^2\omega^{(2)}_{mK}+\cdots,$$
$$\mathbf{h}_{mk}=\mathbf{h}_{mK}+\sum_p(\delta k)a^{(1)}_p\mathbf{h}_{pK}+\sum_p(\delta k)^2a^{(2)}_p\mathbf{h}_{pK}+\cdots, \tag{29}$$

where the superscripts indicate expansion coefficients associated with the indicated powers of δk. We restrict the sums in the second of Eqs. (29) to $p\neq m$; this will yield an $\mathbf{h}_{mk}$ normalized differently than $\mathbf{h}_{mK}$, but as our interest is in the $\omega^{(i)}_{mK}$ this will not be of consequence. Substituting Eqs. (29) into Eq. (28) we find, respectively, for the expressions multiplying $(\delta k)^0$, $(\delta k)^1$, and $(\delta k)^2$,

$$\mathbf{H}_0\cdot\mathbf{h}_{mK}=\omega_{mK}\mathbf{n}\cdot\mathbf{h}_{mK},$$
$$\sum_p a^{(1)}_p(\omega_{pK}-\omega_{mK})\mathbf{n}\cdot\mathbf{h}_{pK}+\mathbf{V}\cdot\mathbf{h}_{mK}=\omega^{(1)}_m\mathbf{n}\cdot\mathbf{h}_{mK}, \tag{30}$$
$$\sum_p a^{(2)}_p(\omega_{pK}-\omega_{mK})\mathbf{n}\cdot\mathbf{h}_{pK}+\sum_p a^{(1)}_p\mathbf{V}\cdot\mathbf{h}_{pK}=\sum_p a^{(1)}_p\omega^{(1)}_m\mathbf{n}\cdot\mathbf{h}_{pK}+\omega^{(2)}_m\mathbf{n}\cdot\mathbf{h}_{mK}.$$

The first of Eqs. (30) is satisfied by assumption [see Eq. (27)]. Taking the dot product of the second of Eqs. (30) with $\mathbf{h}^{\dagger}_{mK}$ and $\mathbf{h}^{\dagger}_{qK}$ $(q\neq m)$, and in each case integrating over z, we find

$$\omega_{mK}^{(1)}=v_{mm}(K),$$
$$a_q^{(1)}=-\frac{v_{qm}(K)}{\omega_{qK}-\omega_{mK}}, \tag{31}$$

respectively, where we have used the orthogonality condition (22) and defined

$$v_{mn}(k)\equiv\frac{\mathbf{h}_{mk}^{\dagger}\cdot\mathbf{V}\cdot\mathbf{h}_{nk}}{N}. \tag{32}$$

Turning to the third of Eqs. (30), take the dot product with $\mathbf{h}_{mK}^{\dagger}$ and integrate over z; we find

$$\sum_p a_p^{(1)}v_{mp}(K)=\omega_{mK}^{(2)} \tag{33}$$

and, using in this the second of Eqs. (31), we obtain

$$\omega_{mK}^{(2)}=-\sum_{p\neq m}\frac{v_{mp}(K)v_{pm}(K)}{\omega_{pK}-\omega_{mK}}. \tag{34}$$

We now have only to note from Eq. (29) that $\omega_{mK}^{(1)}=\partial\omega_{mK}/\partial K$ and $\omega_{mK}^{(2)}=\frac{1}{2}(\partial^2\omega_{mK}/\partial K^2)$ to obtain from Eqs. (31) and (34) the main results of this section:

$$\omega'_{mk}=\frac{\partial\omega}{\partial k}=v_{mm}(k), \tag{35}$$

$$\omega''_{mk}=\frac{\partial^2\omega}{\partial k^2}=-2\sum_{p\neq m}\frac{v_{mp}(k)v_{pm}(k)}{\omega_{pk}-\omega_{mk}}. \tag{36}$$

These expressions for the group velocity and group velocity dispersion (essentially the inverse effective mass) at a point on the photonic band structure (see Fig. 1) are very similar to the corresponding expressions for an electron in a periodic potential [19]. In the latter case the role of $v_{mp}(k)$ is played by a matrix element of the velocity operator; thus we will here refer to the $v_{mp}(k)$ as ''velocity matrix elements.'' With that correspondence the electronic and photonic expressions for the group velocity are identical. The expressions for the group velocity dispersion differ only in that the electronic expression has an extra term due to the mass of the electron. No such term would be expected for a photonic band structure: the only effective mass the photon has is acquired from the lattice. The physical picture of the inverse effective mass associated with a given band (in the electronic case, the lattice contribution thereof) arising from the ''interaction'' of the band with other bands in the lattice follows from the perturbation-theory-like structure of Eq. (36); it is a useful picture in solid state physics and will also be so here. We also note that Eq. (36) for the group velocity dispersion is much simpler than the corresponding expression written in terms of Bloch functions [3], confirming the discussion following Eq. (22).

Inserting the $h_{mk}^{\pm}(z)$ [Eq. (23)] into Eq. (32) for $v_{mn}(k)$, we find

$$\begin{aligned}v_{mn}(k)&=\frac{c}{N}\int_0^L\{[h_{mk}^{+}(z)]^{*}h_{nk}^{+}(z)-[h_{mk}^{-}(z)]^{*}h_{nk}^{-}(z)\}dz\\&=\frac{c}{N}\int_0^L\{[\psi_{mk}^{+}(z)]^{*}\psi_{nk}^{+}(z)-[\psi_{mk}^{-}(z)]^{*}\psi_{nk}^{-}(z)\}dz.\end{aligned} \tag{37}$$

The expression simplifies if we write the $\psi^{\pm}$ in terms of the corresponding Bloch functions ϕ [Eq. (21)]. We find

$$\begin{aligned}\frac{v_{mn}(k)}{c}&=-\frac{1}{2}\frac{ic}{N}\left(\frac{1}{\omega_{mk}}+\frac{1}{\omega_{nk}}\right)\int_0^L\phi_{mk}^{*}(z)\frac{\partial\phi_{nk}}{\partial z}dz\\&=\frac{1}{2}\left(\frac{1}{\omega_{mk}}+\frac{1}{\omega_{nk}}\right)\Omega_{mn}(k),\end{aligned} \tag{38}$$

where

$$\Omega_{mn}(k)\equiv-ic\int_0^d\phi_{mk}^{*}(z)\frac{\partial\phi_{nk}}{\partial z}dz \tag{39}$$

has units of frequency. We have simplified the integral in Eq. (38) by noting that, since the integrand is periodic over d, the integral is simply N $(=L/d)$ times that from 0 to d.

IV. NONLINEARITY AND MULTIPLE SCALES

We now introduce the nonlinear polarization $\mathbf{P}_{\mathrm{NL}}$ through $\mathbf{P}_{\mathrm{NL}}(\vec{r},t)=\hat{\mathbf{x}}P_{\mathrm{NL}}(z,t)$. Instead of Eqs. (2) we find

$$\frac{\partial H}{\partial t}=-\frac{1}{\mu_0}\frac{\partial E}{\partial z},$$
$$\frac{\partial E}{\partial t}=-\frac{1}{\epsilon_0 n^2(z)}\left[\frac{\partial H}{\partial z}+\frac{\partial P_{\mathrm{NL}}}{\partial t}\right] \tag{40}$$

from the Maxwell equations. Taking the same definitions (3) for $A^{\pm}(z,t)$, instead of Eq. (5) we find now

$$i\mathbf{n}\cdot\frac{\partial\mathbf{A}}{\partial t}=\mathbf{M}\cdot\mathbf{A}+\mathbf{B}, \tag{41}$$

where $\mathbf{B}$ has two identical components

$$B^{\pm}(z,t)=-\frac{i}{2\epsilon_0\sqrt{n_0 n(z)}}\frac{\partial P_{\mathrm{NL}}}{\partial t}. \tag{42}$$

Adopting a simple model for $P_{\mathrm{NL}}(z,t)$ as resulting from a nondispersive, third-order nonlinearity, we set [14,15]

$$P_{\mathrm{NL}}(z,t)=\epsilon_0\chi^{(3)}(z)E^3(z,t), \tag{43}$$

where $\chi^{(3)}(z)$, if not uniform, varies with the same period as $n(z)$, $\chi^{(3)}(z+d)=\chi^{(3)}(z)$. Expressing $E(z,t)$ in terms of $A^{\pm}(z,t)$ from Eqs. (3), Eq. (42) becomes

$$B^{\pm}(z,t)=-\frac{in_0}{2}\frac{\chi^{(3)}(z)}{n^2(z)}\frac{\partial}{\partial t}\{[A^{+}(z,t)+A^{-}(z,t)]^3\}. \tag{44}$$

In the presence of this nonlinearity, Eq. (41) is not satisfied by a solution of the form (15). We shall construct approximate solutions of Eq. (41) by allowing the $f_\mu = f_{mk}$ in Eq. (15) to become slowly varying in both space and time, in a sense to be described below. In the examples we present here there will be either one or two large components $f_{mk}(z,t)$; these we call *principal* components of the solution [3]. The electromagnetic field thus consists mainly of one, or of the sum of two, Bloch function modulated by ''envelope functions'' $f_{mk}(z,t)$.

Consider now the solution that would result, *even in the absence of nonlinearity*, if we put only such principal components into Eq. (15) with $f_{mk}(z,t=0)$ not uniform but describing, say, a wave packet. We would expect that, to good approximation, the solution could be described by the $f_{mk}(z,t)$ acquiring a time dependence; indeed, we would expect the time dependence to involve the motion of the wave packet(s) with group velocity ω'_{mk} dispersing as described by ω''_{mk} and, if described in great enough detail, with even more wave packet reshaping. This we confirm below. We also find that components f_{pk} for Bloch functions other than those making up the principal components are also generated, although they are smaller in magnitude; these we call *companion* components [3]. If a weak nonlinearity is now introduced, the only modification of this scenario is in the details of the evolution of the amplitudes $f_{qk}(z,t)$ for the principal and companion components. Of course, there is a qualitative difference between the linear and nonlinear problems: In the linear case the evolution of a field specified initially by one or two nonuniform $f_{mk}(z,t=0)$ could always be determined by rewriting that field, according to Eq. (15) at $t=0$, as a sum over an infinite number of *uniform* f_{qk}; the subsequent field would follow then from Eq. (15) at $t>0$. Such a method of solution is of course not possible in the presence of nonlinearity.

To keep track in a careful way of the ''weak'' nonlinearity and ''slowly varying'' amplitudes alluded to above we introduce a small parameter $\eta \ll 1$. A typical function of interest is then written as

$$f(z,t) = F(z, \eta z, \eta^2 z, \ldots; t, \eta t, \eta^2 t, \ldots), \tag{45}$$

where F is assumed to vary equally significantly as each of its spatial arguments varies over a given range d and each of its temporal arguments varies over a given period τ. Then the variation of f over different length and time scales is captured by the variation of F on its different parameters. The ranges $\eta^p d$ and periods $\eta^p \tau$, $p=0,1,2,\ldots$, define the *multiple scales* of the problem [23]. Setting

$$z_p = \eta^p z, \qquad t_p = \eta^p t, \tag{46}$$

we have

$$f(z,t) = F(z_0, z_1, z_2, \ldots; t_0, t_1, t_2, \ldots) \tag{47}$$

and

$$\frac{\partial f}{\partial z} = \frac{\partial F}{\partial z_0} + \eta \frac{\partial F}{\partial z_1} + \eta^2 \frac{\partial F}{\partial z_2} + \ldots, \qquad \frac{\partial f}{\partial t} = \frac{\partial F}{\partial t_0} + \eta \frac{\partial F}{\partial t_1} + \eta^2 \frac{\partial F}{\partial t_2} + \ldots \tag{48}$$

explicitly exhibiting the variation of f over the multiple scales. Sometimes not all the scales appear and sometimes forms more general than Eq. (47) are employed. In particular, for the case of a single principal component we seek an approximate solution of the form

$$\mathbf{A} = \left[f_{mk}(z,t)\boldsymbol{\Psi}_{mk} + \sum_{p \neq m} f_{pk}(z,t)\boldsymbol{\Psi}_{pk} \right] e^{-i\omega_{mk}t} + \text{c.c.}, \tag{49}$$

where c.c. indicates the complex conjugate. Further, we take here $\tau = 2\pi/\omega_{mk}$ and d to be the period of the lattice, corresponding to the fastest time and length scales in the problem, respectively. To simplify later expressions we introduce a factor a to characterize a typical amplitude of the fields we wish to treat; it is set such that the $F^{(i)}_{qk}$ that appear below are dimensionless and of order unity. Furthermore, we take $f_{qk}(z,t)$ of the form

$$f_{mk}(z,t) = a F^{(0)}_{mk}(z_1, z_2, \ldots; t_1, t_2, \ldots), \tag{50}$$

$$f_{pk}(z,t) = a\,\eta F^{(1)}_{pk}(z_1, z_2, \ldots; t_1, t_2, \ldots) + a\,\eta^2 F^{(2)}_{pk}(z_1, z_2, \ldots; t_1, t_2, \ldots) + \ldots$$

for $p \neq m$. Note that the companion components ($p \neq m$) contain terms that are smaller than the primary component by powers of the same parameter η that separates the different length and time scales. The absence of a dependence of $F^{(0)}_{mk}$ on z_0 and t_0 might be guessed from the spirit of the approach: The rapid variation on these fundamental scales is all contained in $\boldsymbol{\Psi}_{mk}$ and $e^{-i\omega_{mk}t} = e^{-i\omega_{mk}t_0}$ [Eq. (49)], respectively. Nonetheless, the validity of ansatz (49) is, in the end verified by our ability to construct solutions of the assumed form (see Secs. V and VI).

The procedure described above is implemented by inserting a form such as Eq. (49) in the nonlinear equations (41), using expressions such as Eq. (48) to evaluate the derivatives, and then constructing the equations that must be satisfied for Eq. (41) to be satisfied to successive powers of η. This protocol is facilitated by noting that, since $n(z) = n(z_0)$, we can write $\mathbf{M}$ [Eq. (7)] as

$$\mathbf{M} = \mathbf{M}^{(0)} - i\eta \mathbf{V} \frac{\partial}{\partial z_1} - i\eta^2 \mathbf{V} \frac{\partial}{\partial z_2} + \cdots, \tag{51}$$

where $\mathbf{V}$ is given by Eq. (26) and

$$\mathbf{M}^{(0)} = \begin{bmatrix} -ic\dfrac{\partial}{\partial z_0} & \dfrac{1}{2}ic\left(\dfrac{\partial \ln n(z_0)}{\partial z_0}\right) \\ -\dfrac{1}{2}ic\left(\dfrac{\partial \ln n(z_0)}{\partial z_0}\right) & ic\dfrac{\partial}{\partial z_0} \end{bmatrix} \tag{52}$$

involves only z_0 and $\partial/\partial z_0$. Equation (41) then becomes

$$i\mathbf{n}\cdot\left[\frac{\partial}{\partial t_0}+\eta\frac{\partial}{\partial t_1}+\eta^2\frac{\partial}{\partial t_2}+\cdots\right]\mathbf{A}$$
$$=\left[\mathbf{M}^{(0)}-i\eta\mathbf{V}\frac{\partial}{\partial z_1}-i\eta^2\mathbf{V}\frac{\partial}{\partial z_2}-\cdots\right]\cdot\mathbf{A}+\mathbf{B}. \tag{53}$$

Since we wish to solve this equation in successive powers of η, we obviously must relate the nonlinearity to η. Setting

$$\chi^{(3)}(z)=\chi_{\mathrm{NL}}\gamma(z), \tag{54}$$

where $\gamma(z)$ is of order unity and dimensionless, the dimensionless quantity $\chi_{\mathrm{NL}}a^2$ can be taken as characterizing the ''strength'' of the nonlinearity. If the physical nonlinearity and intensities of interest are such that $\chi_{\mathrm{NL}}a^2$ is of order η^s, where $s=1,2,\ldots$, we say that the *intensity index* is s. Then the leading term in $\mathbf{B}$ will be of order η^s. By satisfying Eq. (53) to higher and higher powers of η we generally expect to get equations that better and better capture the exact solution, at least in an asymptotic sense with respect to η. But we will never press the analysis beyond η^s, because Eq. (43) itself is an approximation to the nonlinear response; going beyond η^s without including higher-order nonlinearities would, in general, be inconsistent.

In discussions of multiple-scale analyses such as these, η is often set equal to unity at the end of the calculation, following a similar cavalier approach sometimes taken in perturbation theory. We will be more careful here because the restriction that the F's [see Eq. (47)] vary equally significantly as each of their parameters of a given type (spatial or temporal) varies over a given range, and the condition $\eta\ll 1$, in fact determine the set of conditions over which the equations we derive are valid; this we wish to sketch and show how the range of validity of the equations could be in fact determined for a given set of parameters. We now turn to the derivation of those equations.

V. SINGLE PRINCIPAL COMPONENT

Following the approach described in Sec. IV, we now establish the equations that the principal and companion components of $\mathbf{A}$ must satisfy if we are to have a good approximation to a solution of the full nonlinear equation (41). We begin with the ansatz (49) for the field $\mathbf{A}$, proceeding under the assumption that the F_{qk} are of order unity and only vary significantly as each of their spatial arguments range over distances of order or much greater than d and as each of their temporal arguments range over times of order or much greater than $\tau\equiv 2\pi/\omega_{mk}$. The equations that are then derived for the F_{qk} can be considered good approximate descriptions of the dynamics as long as their solutions are indeed found to satisfy these requirements, which we refer to as ''*consistency conditions.*''

A. Intensity index $s\geqslant 3$: Schrödinger equation

To begin the process we must set the parameter η. If $f_{mk}(z,t=0)$ varies over a length of order $\Lambda\gg d$, then the simplest approach is to identify this variation with the scale z_1; it follows that $|\eta a(\partial F^{(0)}_{mk}/\partial z_1)|\simeq|f_{mk}(z,t=0)/\Lambda|\simeq|aF^{(0)}_{mk}/\Lambda|$ and we can establish $|\partial F^{(0)}_{mk}/\partial z_1|\leqslant|F^{(0)}_{mk}/d|$ as required if we set $\eta\geqslant d/\Lambda$. This establishes a lower limit for η; upper limits for η are set by the condition $\eta\ll 1$ required for a physically meaningful expansion in powers of η and certain other conditions mentioned below. We will find it necessary to set $\eta\simeq gd/\Lambda$, where $g>1$ and is to be specified later, to treat the range of situations of interest.

To concentrate first on the linear aspects of the dynamics, we assume that the nonlinearity is sufficiently weak that the intensity index $s\geqslant 3$; such a result could of course follow from a small physical nonlinearity or a small amplitude of $f_{mk}(z,t=0)$ or both. Then, putting Eq. (49) into the exact Eq. (53), the nonlinearity does not enter until we consider powers of η greater than or equal to 3. First note that Eq. (53) is satisfied to order η^0 because

$$\mathbf{M}^{(0)}\cdot\boldsymbol{\Psi}_{mk}=\omega_{mk}\mathbf{n}\cdot\boldsymbol{\Psi}_{mk} \tag{55}$$

[cf. Eq. (9)], which holds since $\boldsymbol{\Psi}_{mk}$ depends only on $z=z_0$. To be satisfied to order η^1, we find that Eq. (53) requires the condition

$$i\frac{\partial F^{(0)}_{mk}}{\partial t_1}\mathbf{n}\cdot\boldsymbol{\Psi}_{mk}=-i\frac{\partial F^{(0)}_{mk}}{\partial z_1}\mathbf{V}\cdot\boldsymbol{\Psi}_{mk}$$
$$+\sum_{q\neq m}F^{(1)}_{qk}(\omega_{qk}-\omega_{mk})\mathbf{n}\cdot\boldsymbol{\Psi}_{qk}, \tag{56}$$

while to be satisfied to order η^2 Eq. (53) requires the condition

$$i\frac{\partial F^{(0)}_{mk}}{\partial t_2}\mathbf{n}\cdot\boldsymbol{\Psi}_{mk}+i\sum_{q\neq m}\frac{\partial F^{(1)}_{qk}}{\partial t_1}\mathbf{n}\cdot\boldsymbol{\Psi}_{qk}$$
$$=-i\frac{\partial F^{(0)}_{mk}}{\partial z_2}\mathbf{V}\cdot\boldsymbol{\Psi}_{mk}+\sum_{q\neq m}\left[F^{(2)}_{qk}(\omega_{qk}-\omega_{mk})\mathbf{n}\right.$$
$$\left.-i\frac{\partial F^{(1)}_{qk}}{\partial z_1}\mathbf{V}\right]\cdot\boldsymbol{\Psi}_{qk}. \tag{57}$$

From each of Eqs. (56) and (57) we get an equation for each band index p by taking the dot product with $\boldsymbol{\Psi}^{\dagger}_{pk}$ and integrating over all z_0, which, in the spirit of this approach, is treated as a variable independent of the other z_r, $r\geqslant 1$. From Eq. (56), for $q,p\neq m$, we find

$$F^{(1)}_{pk}=\frac{iv_{pm}(k)}{\omega_{pk}-\omega_{mk}}\frac{\partial F^{(0)}_{mk}}{\partial z_1}, \tag{58}$$

where we have used Eq. (32) for the velocity matrix element $v_{pm}(k)$; for $p=m$ we find

$$i\frac{\partial F^{(0)}_{mk}}{\partial t_1}=-i\omega'_{mk}\frac{\partial F^{(0)}_{mk}}{\partial z_1}, \tag{59}$$

where we have used Eq. (35) for the group velocity ω'_{mk}. From Eq. (57) we can find an equation for $F^{(2)}_{pk}$ corresponding to Eq. (58), which we will not write down; the equation corresponding to Eq. (59) is found to be [3]

$$i\frac{\partial F_{mk}^{(0)}}{\partial t_2} = -i\omega'_{mk}\frac{\partial F_{mk}^{(0)}}{\partial z_2} - i\sum_{p\neq m} v_{mp}(k)\frac{\partial F_{pk}^{(1)}}{\partial z_1}$$

$$= -i\omega'_{mk}\frac{\partial F_{mk}^{(0)}}{\partial z_2} - \frac{1}{2}\omega''_{mk}\frac{\partial^2 F_{mk}^{(0)}}{\partial z_1^2}, \tag{60}$$

where in the second form of Eq. (60) we have used Eq. (58) for $F_{pk}^{(1)}$ and Eq. (35) for the group velocity dispersion.

Before proceeding we examine the consistency conditions, at $t=0$, to which these equations are subject. Consider first Eq. (59); we require $|\partial F_{mk}^{(0)}/\partial t_1| \leqslant |F_{mk}^{(0)}/\tau| = \omega_{mk}|F_{mk}^{(0)}|/2\pi$ and, since $|\partial F_{mk}^{(0)}/\partial z_1| \simeq |F_{mk}^{(0)}|/gd$ [see the discussion before Eq. (55)], the condition gives

$$\left|\frac{\omega'_{mk}}{\omega_{mk}/k_G}\right| \leqslant g \tag{61}$$

or, equivalently,

$$\left|\frac{\omega'_{mk}}{\omega_{mk}/k}\right| \leqslant g\left|\frac{k}{k_G}\right|, \tag{62}$$

where $k_G \equiv 2\pi/d$ is a reciprocal lattice vector of the grating. Equation (61) is easy to satisfy near $|k|=\pi/d$ or $k=0$ (except on the lowest branch of the dispersion relation where $\omega_{mk}=0$ at $k=0$) since there $\omega'_{mk}\simeq 0$. Intermediate between these extreme values we have $|\omega'_{mk}|\simeq|\omega_{mk}/k|$ on the lowest branch and a g significantly greater than unity is required to satisfy Eq. (62); for higher branches this is less difficult, for there $|\omega'_{mk}|<|\omega_{mk}/k|$. To proceed we must assume that, for our initial conditions, a g can be found satisfying Eq. (62) for the Bloch function of interest, while still maintaining $\eta = gd/\Lambda \ll 1$.

Turning now to Eq. (58), the consistency condition that $F_{pk}^{(1)}$ is of order unity or less, given that $F_{mk}^{(0)}$ is of order unity, requires

$$\left|\frac{v_{pm}(k)}{(\omega_{pk}-\omega_{mk})d}\right| \leqslant g \tag{63}$$

for all $p\neq m$. Once the Bloch states of a band structure are evaluated, the left-hand side of Eq. (63) can be calculated using Eq. (38). Typically, though, for g not too large Eq. (63) is easiest satisfied at k away from 0 and π/d; i.e., it most generally holds at points on the dispersion relation where all other bands are ''remote'' from the band providing the principal component (see Fig. 1). Next, the consistency condition resulting from Eq. (60) is

$$\left|\frac{\omega''_{mk}k_G^2}{\omega_{mk}}\right| \leqslant 4\pi g^2, \tag{64}$$

which is again easiest to satisfy, for g not too large, if all bands are remote from band m at point k on the dispersion relation. A similar result follows from the consistency condition following from the equation for $F_{pk}^{(2)}$ mentioned above. Thus the development of this section is quite generally dependent on the condition of all bands other than that providing the principal component being remote, in a form that is made precise by the equations given above. A development that can be used when such a condition is not satisfied is presented in Sec. VI.

Note that we have only discussed the consistency conditions at $t=0$. As the $F_{qk}^{(i)}$ evolve according to Eqs. (58)–(60), the resulting **A** [Eq. (49)] constitutes a good approximate solution only as long as the consistency conditions remain satisfied; this of course must be investigated on a case-by-case basis by examining the solutions in detail.

But let us now assume that at least for some length of time the consistency conditions are satisfied. We can simplify our results [Eqs. (58)-(60)] by noting that, if we stop the development at order η^2, we have to this order

$$i\eta\frac{\partial}{\partial t_1} + i\eta^2\frac{\partial}{\partial t_2} = i\frac{\partial}{\partial t}, \tag{65}$$

$$i\eta\frac{\partial}{\partial z_1} + i\eta^2\frac{\partial}{\partial z_2} = i\frac{\partial}{\partial z},$$

$$\eta^2\frac{\partial^2}{\partial z_1^2} = \frac{\partial^2}{\partial z^2}$$

for functions that do not depend on z_0 or t_0. Then, combining Eqs. (59) and (60) we find

$$i\frac{\partial f_{mk}}{\partial t} + i\omega'_{mk}\frac{\partial f_{mk}}{\partial z} + \frac{1}{2}\omega''_{mk}\frac{\partial^2 f_{mk}}{\partial z^2} = 0 \tag{66}$$

[refer to Eqs. (49) and 50)], while Eq. (58) and the corresponding equation for $F_{pk}^{(2)}$ can be combined to write f_{pk} $(p\neq m)$ in terms of derivatives of f_{mk}. Hence follows the name companion component: Once f_{mk} is determined by solving Eq. (66), the other f_{pk} can be found immediately; this will quite generally be the situation in the examples presented in this paper. Note that no nonlinear effects appear, to this order, because we have assumed the intensity index $s\geqslant 3$. Equation (66) does, however, describe a wave packet traveling with group velocity ω'_{mk} and dispersing with group velocity dispersion ω''_{mk}; with a change of variables to a moving frame $\bar{t}\equiv t$, $\bar{z}\equiv z-\omega'_{mk}t$, Eq. (66) becomes

$$i\frac{\partial f_{mk}}{\partial \bar{t}} + \frac{1}{2}\omega''_{mk}\frac{\partial^2 f_{mk}}{\partial \bar{z}^2} = 0, \tag{67}$$

a Schrödinger equation. The general pattern of the expansion is now clear. Just as higher powers of **V** in the $\mathbf{k}\cdot\mathbf{V}$ expansion (Sec. III) lead to higher derivatives of ω_{mk} with respect to k [see Eq. (29)], higher powers of η lead, through successive $\partial^p/\partial z^p$ in Eq. (53), to higher derivatives of the ''envelope function'' f_{mk} premultiplied by higher derivatives of ω_{mk} with respect to k. Thus, once the expected pattern is identified, corrections to Eq. (66) can be written down ''by hand,'' without going through the detailed analysis. Strictly speaking, if the analysis is stopped at a given power of η, the consistency conditions should be checked (at least) at the next highest order; we shall not outline that explicitly here.

B. Intensity index $s=2$: Nonlinear Schrödinger equation

Although the result (66) is certainly not unexpected on physical grounds, the effort in establishing it is justified in that the development we have presented allows a careful inclusion of the effects of nonlinearity. Suppose, for example, we now assume the intensity index $s=2$. Then nonlinear effects enter at the order of η^2 that we have presented here. To see their effect we must return to Eqs. (44). Since to lowest order in η we have

$$A^{\pm}(z,t)=aF_{mk}^{(0)}\psi_{mk}^{\pm}(z_0)e^{-i\omega_{mk}t_0}+\text{ c.c.} \tag{68}$$

[see Eqs. (49) and (50)], we have to this order

$$A^{+}(z,t)+A^{-}(z,t)=aF_{mk}^{(0)}\sqrt{n(z_0)}\,\phi_{mk}(z_0)e^{-i\omega_{mk}t_0}+\text{c.c.} \tag{69}$$

[see Eq. (21)]. Thus, from Eq. (44), for the components of **B** we find

$$B^{\pm}(z,t)=\beta(z_0)a^3|F_{mk}^{(0)}|^2F_{mk}^{(0)}e^{-i\omega_{mk}t_0}+\text{c.c.}, \tag{70}$$

where

$$\beta(z_0)=-\frac{3}{2}n_0\omega_{mk}\frac{a^3\chi^{(3)}(z_0)}{\sqrt{n(z_0)}}\phi_{mk}^2(z_0)\phi_{mk}^{*}(z_0). \tag{71}$$

In writing down Eq. (70) we have neglected terms that vary as $e^{\pm 3i\omega_{mk}t_0}$; these we discuss at the end of this section.

In the presence of nonlinearity with an intensity index $s=2$, the analysis leading to Eqs. (56) and (57) leaves Eq. (56) unchanged, since it results from order η^1. But we find a new equation in place of Eq. (57). It is given by Eq. (57) with the term $\eta^{-2}a^{-1}\mathbf{B}$ added to its right-hand side, where **B** is replaced by its approximation (70) above; our assumption of an intensity index $s=2$ guarantees that this term is of order unity [see the discussion following Eq. (54)]. Since Eq. (56) is unchanged we still obtain

$$i\frac{\partial F_{mk}^{(0)}}{\partial t_1}=-i\omega_{mk}'\frac{\partial F_{mk}^{(0)}}{\partial z_1} \tag{72}$$

[cf. Eq. (59)], but by taking the dot product of the new version of Eq. (57) with $\mathbf{\Psi}_{mk}^{\dagger}$ we find a new equation for $\partial F_{mk}^{(0)}/\partial t_2$,

$$i\frac{\partial F_{mk}^{(0)}}{\partial t_2}=-i\omega_{mk}'\frac{\partial F_{mk}^{(0)}}{\partial z_2}-\frac{1}{2}\omega_{mk}''\frac{\partial^2 F_{mk}^{(0)}}{\partial z_1^2}+\frac{(\mathbf{\Psi}_{mk}^{\dagger}\cdot\hat{\mathbf{B}})e^{i\omega_{mk}t_0}}{\eta^2 aN}, \tag{73}$$

where we use the parentheses notation of Sec. II [see Eq. (12)] to denote an integral over z_0; $\hat{\mathbf{B}}$ denotes the positive-frequency part of **B**, with respect to t_0, as approximated by Eq. (70) [cf. our sign convention in Eq. (49)]. The new term in Eq. (73) involves

$$\begin{aligned}(\mathbf{\Psi}_{mk}^{\dagger}\cdot\hat{\mathbf{B}})e^{i\omega_{mk}t_0}&=|F_{mk}^{(0)}|^2F_{mk}^{(0)}\int_0^L[\psi_{mk}^{+}(z_0)\\&\quad+\psi_{mk}^{-}(z_0)]^{*}\beta(z_0)dz_0\\&=|F_{mk}^{(0)}|^2F_{mk}^{(0)}\int_0^L\sqrt{n(z_0)}\,\phi_{mk}^{*}(z_0)\beta(z_0)dz_0,\end{aligned} \tag{74}$$

where we have used Eq. (21). Using the periodicity of the Bloch functions and the form (71) of $\beta(z_0)$, we find

$$\frac{(\mathbf{\Psi}_{mk}^{\dagger}\cdot\hat{\mathbf{B}})e^{i\omega_{mk}t_0}}{N}=-a^3\alpha|F_{mk}^{(0)}|^2F_{mk}^{(0)}, \tag{75}$$

where

$$\alpha=\frac{3}{2}n_0\omega_{mk}\int_0^d\chi^{(3)}(z_0)|\phi_{mk}(z_0)|^4dz_0 \tag{76}$$

characterizes how the Bloch function $\phi_{mk}(z_0)$ effectively ''samples'' the distribution of the nonlinearity over the unit cell. Using Eq. (75) in Eq. (73) and combining that with Eq. (72) using Eqs. (65), we find that if we stop our analysis at order η^2 we obtain the equation

$$i\frac{\partial f_{mk}}{\partial t}+i\omega_{mk}'\frac{\partial f_{mk}}{\partial z}+\frac{1}{2}\omega_{mk}''\frac{\partial^2 f_{mk}}{\partial z^2}+\alpha|f_{mk}|^2f_{mk}=0, \tag{77}$$

where the nonlinear term now [cf. Eq. (66)] appears at the order of the group velocity dispersion term. In the moving frame discussed after Eq. (66) this equation becomes

$$i\frac{\partial f_{mk}}{\partial\overline{t}}+\frac{1}{2}\omega_{mk}''\frac{\partial^2 f_{mk}}{\partial\overline{z}^2}+\alpha|f_{mk}|^2f_{mk}=0, \tag{78}$$

a nonlinear Schrödinger equation. This is in agreement with a previously derived result [3]; the formal difference in the definition of α between the two is due only to the fact that we here have derived the equation for the principal component envelope function $f_{mk}(z,t)$ that modulates the components of **A** [cf. Eq. (49)]. In earlier work the envelope function was the function that modulated the Bloch function in the principal component of $E(z,t)$. The latter differs from the former by a factor of $\sqrt{n_0}$, as can be confirmed by using Eq. (49), together with the equation relating the components of $A^{\pm}(z,t)$ and $E(z,t)$ [Eq. (3)] and the equation relating $\psi_{mk}^{\pm}(z)$ and $\phi_{mk}(z)$ [Eq. (21)].

Note that Eq. (77) is identical in form to what one finds in a weakly nonlinear material with no periodicity in its linear properties, but with material dispersion; here it is simply that the grating structure, rather than the underlying material dispersion, provides the ω_{mk}'' term. Inasmuch as we only have one principal component in our expansion (49) and (50) the development presented here leads to only one *dynamical quantity* f_{mk}. The amplitudes of the other f_{pk} are ''slaved'' to f_{mk} as companion components [Eq. (58)]; nonetheless, they affect the dynamics of f_{mk} through the curvature term appearing in the equations above, manifesting the ''contribu-

tion'' of the other bands to the effective mass of the band providing the principal component (see the discussion at the end of Sec. III).

If we have a stronger nonlinearity (suppose the intensity index $s=1$), then if we repeat the above analysis but stop at order η^1 we find, in the case considered here of all other bands being remote,

$$i\frac{\partial f_{mk}}{\partial t}+i\omega'_{mk}\frac{\partial f_{mk}}{\partial z}+\alpha|f_{mk}|^2 f_{mk}=0. \tag{79}$$

In the moving frame used above, there is only self-phase modulation. For such a strong nonlinearity ($s=1$), it would, in general, be inconsistent to add in the group velocity dispersion term (order η^2) since, as discussed after Eq. (54), terms from higher-order physical nonlinearities could be expected to enter as well at that level, in combination with higher-order contributions from the assumed $\chi^{(3)}$ nonlinearity.

We close this section with a comment on the neglected third-harmonic terms [see comments after Eq. (70)]. If such terms are included, then in expressions for the companion component amplitudes, contributions with resonant denominators $(\omega_{pk}-3\omega_{mk})$ appear rather than with the denominator $(\omega_{pk}-\omega_{mk})$ [cf. Eq. (58)] that appears at lowest order. It is certainly possible to have an $\omega_{pk}\simeq 3\omega_{mk}$, and in such a case the formal analysis presented here fails and one must in fact develop a theory involving coupled nonlinear Schrödinger equations, as has been done in another formalism earlier [24]. Even in the presence of such formal ''resonances,'' however, one can often be saved from this difficulty by physical considerations. We have assumed here that the underlying material is nondispersive, and while this may be a reasonable approximation for frequencies ω close to ω_{mk}, it often is not over frequency ranges extending to $\omega\simeq 3\omega_{mk}$. Thus the band structure formally derived at such frequencies, and indeed the assumption of no absorption there, may well be in error [24]. Although a detailed analysis has not been performed, we can expect on physical grounds that in many instances the actual material dispersion and absorption may obviate the difficulties associated with the above-mentioned possible resonant denominators and render the description here based on the neglect of third-harmonic generation adequate.

VI. TWO PRINCIPAL COMPONENTS

A. Intensity index $s\geq 3$: Coupled-envelope-function equations with remote band effects

We now turn to approximate solutions of Eqs. (40) involving frequencies over ranges where the assumption that all but one band is remote from the frequencies of interest is not valid. The most striking and interesting of such cases is when the frequencies of interest are near a band gap (see Fig. 1). Labeling the upper and lower frequencies at that gap by ω_u and ω_l, respectively, for frequencies in the neighborhood of $\omega_0\equiv 1/2(\omega_u+\omega_l)$ we must expect that the functions $\mathbf{\Psi}_u$ and $\mathbf{\Psi}_l$, associated with ω_u and ω_l, respectively, both contribute significantly to the field $\mathbf{A}$. Thus, instead of an $\mathbf{A}$ of the form specified by Eqs. (49) and (50), we look for a field of the form

$$\mathbf{A}=\left[f_u(z,t)\mathbf{\Psi}_u+f_l(z,t)\mathbf{\Psi}_l+\sum_{p\neq u,l}f_p(z,t)\mathbf{\Psi}_p\right]e^{-i\omega_0 t_0}+\text{c.c.}, \tag{80}$$

where

$$\begin{aligned} f_{u,l}(z,t)&=aF^{(0)}_{u,l}(z_1,z_2,\ldots t_1,t_2,\ldots),\\ f_p(z,t)&=a\eta F^{(1)}_p(z_1,z_2,\ldots;t_1,t_2,\ldots)\\ &\quad+a\eta^2F^{(2)}_p(z_1,z_2,\ldots;t_1,t_2,\ldots)+\ldots \end{aligned} \tag{81}$$

for $p\neq u,l$. We drop the k label at this point; $k=0$ or $k=\pi/d$ at a band gap and all the Bloch functions involved in the sum (80) are at whichever of these k's is associated with the gap of interest. Our η can be chosen as discussed at the start of Sec. V, with the principal components $F^{(0)}_{u,l}$ playing the role there played by $F^{(0)}_{mk}$; it will become clear that, since $\omega'_u=\omega'_l=0$ at a band gap, an $\eta\simeq d/\Lambda$ will here be generally sufficient [cf. Eqs. (61) and (62)]. We will see that significant coupling between the amplitudes $f_u(z,t)$ and $f_l(z,t)$ occurs when $\Delta\equiv\omega_u-\omega_l$ is of order $\eta\omega_0$ (or smaller); we assume this here.

We proceed by inserting Eq. (80) into the exact Eq. (53) and identifying the coefficients of different powers of η. We begin by assuming that the intensity index $s\geq 3$, as we did at the start of Sec. V. Then the nonlinearity does not enter to order η^2 in the expansion, which is as far as we shall go. Note, however, an important difference between the development here and in Sec. V: Here

$$i\mathbf{n}\cdot\frac{\partial\mathbf{A}_P}{\partial t_0}\neq\mathbf{M}^{(0)}\cdot\mathbf{A}_P, \tag{82}$$

where $\mathbf{A}_P$ denotes the principal components of $\mathbf{A}$. The assumed form of $\mathbf{A}$ has a t_0 dependence characterized by frequency ω_0, which is neither the eigenfrequency of $\mathbf{\Psi}_u$ nor $\mathbf{\Psi}_l$. But, because Δ is of order $\eta\omega_0$, the difference in the two terms in Eq. (82) generates contributions of order η^1. Setting

$$\begin{aligned} \omega_u-\omega_0&\equiv\eta\sigma_u,\\ \omega_l-\omega_0&\equiv\eta\sigma_l, \end{aligned} \tag{83}$$

where $\sigma_{u,l}$ are of order ω_0, Eq. (53) is satisfied to order η^0; for it to be satisfied to order η^1 we require

$$\begin{aligned} i\mathbf{n}\cdot\left[\frac{\partial F^{(0)}_u}{\partial t_1}\mathbf{\Psi}_u+\frac{\partial F^{(0)}_l}{\partial t_1}\mathbf{\Psi}_l\right]&=\mathbf{n}\cdot[\sigma_u F^{(0)}_u\mathbf{\Psi}_u+\sigma_l F^{(0)}_l\mathbf{\Psi}_l]\\ &\quad-i\mathbf{V}\cdot\left[\frac{\partial F^{(0)}_u}{\partial z_1}\mathbf{\Psi}_u+\frac{\partial F^{(0)}_l}{\partial z_1}\mathbf{\Psi}_l\right]\\ &\quad+\sum_{q\neq u,l}\mathbf{n}\cdot\mathbf{\Psi}_q F^{(1)}_q(\omega_q-\omega_0) \end{aligned} \tag{84}$$

and for it to be satisfied to order η^2 we require

$$i\mathbf{n}\cdot\left[\frac{\partial F_u^{(0)}}{\partial t_2}\boldsymbol{\Psi}_u+\frac{\partial F_l^{(0)}}{\partial t_2}\boldsymbol{\Psi}_l\right]+i\sum_{q\neq u,l}\frac{\partial F_q^{(1)}}{\partial t_1}\mathbf{n}\cdot\boldsymbol{\Psi}_q$$
$$=-i\mathbf{V}\cdot\left[\frac{\partial F_u^{(0)}}{\partial z_2}\boldsymbol{\Psi}_u+\frac{\partial F_l^{(0)}}{\partial z_2}\boldsymbol{\Psi}_l\right]$$
$$+\sum_{q\neq u,l}\left[\mathbf{n}F_q^{(2)}(\omega_q-\omega_0)-i\frac{\partial F_q^{(1)}}{\partial z_1}\mathbf{V}\right]\cdot\boldsymbol{\Psi}_q. \quad (85)$$

As in Sec. V, we now take the dot product of these equations with $\boldsymbol{\Psi}_p^\dagger$ for each p and integrate over z_0. From Eq. (84) we find, for $p\neq u,l$, that we require

$$F_p^{(1)}=\frac{iv_{pu}}{\omega_p-\omega_0}\frac{\partial F_u^{(0)}}{\partial z_1}+\frac{iv_{pl}}{\omega_p-\omega_0}\frac{\partial F_l^{(0)}}{\partial z_1}, \quad (86)$$

while for $p=u,l$ we find, respectively,

$$i\frac{\partial F_u^{(0)}}{\partial t_1}=\sigma_u F_u^{(0)}-iv_{ul}\frac{\partial F_l^{(0)}}{\partial z_1},$$
$$i\frac{\partial F_l^{(0)}}{\partial t_1}=\sigma_l F_l^{(0)}-iv_{lu}\frac{\partial F_u^{(0)}}{\partial z_1}. \quad (87)$$

Here v_{ij} corresponds to the velocity matrix element [cf. Eqs. (38) and (39)] between the states $\mathbf{h}_i$ and $\mathbf{h}_j$ at the k associated with the band gap of interest. Equations (86) and (87) should be compared with the corresponding Eqs. (58) and (59) of Sec. V. Since $\omega_u'=\omega_l'=0$ at a band gap, there is nothing on the right-hand side of Eq. (87) corresponding to the right-hand side of Eq. (59). Rather, here, there is, to order η^1, a coupling between the $F_u^{(0)}$ and $F_l^{(0)}$ because of the closeness of the eigenfrequencies ω_u and ω_l; formally, each of these is also ''coupled to itself'' because ω_0 is used as the common reference frequency of the field **A**. From Eq. (86) we see that here all bands *other* than u and l must be remote, in the sense discussed in Sec. V concerning the corresponding Eq. (58), for the expansion in powers of η to be valid.

Turning now to Eq. (85), putting the equation into $\boldsymbol{\Psi}_u^\dagger$ and $\boldsymbol{\Psi}_l^\dagger$ and integrating over z_0 yields

$$i\frac{\partial F_u^{(0)}}{\partial t_2}=-iv_{ul}\frac{\partial F_l^{(0)}}{\partial z_2}-i\sum_{p\neq u,l}v_{up}\frac{\partial F_p^{(1)}}{\partial z_1}, \quad (88)$$
$$i\frac{\partial F_l^{(0)}}{\partial t_2}=-iv_{lu}\frac{\partial F_u^{(0)}}{\partial z_2}-i\sum_{p\neq u,l}v_{lp}\frac{\partial F_p^{(1)}}{\partial z_1}.$$

Compare this with the corresponding equation (60) in Sec. V. Using Eq. (86) in Eq. (88), it is clear that the expression involves the terms

$$\tilde{\omega}_u''\equiv-2\sum_{p\neq u,l}\frac{v_{up}v_{pu}}{\omega_p-\omega_0}, \quad (89)$$
$$\tilde{\omega}_l''\equiv-2\sum_{p\neq u,l}\frac{v_{lp}v_{pl}}{\omega_p-\omega_0}.$$

Except for the appearance in the denominators of ω_0, rather than ω_u and ω_l, respectively, these are the contributions to the dispersion at the band gap of the bands u and l, other than that which can be associated with their interaction with each other, as described in the $\mathbf{k}\cdot\mathbf{V}$ expansion of Sec. III. Combining then Eqs. (87) and (88) and using the expressions (65) valid to order η^2, we find to that order that the envelope functions $f_u(z,t)$ and $f_l(z,t)$ satisfy

$$i\frac{\partial f_u}{\partial t}-\frac{\Delta}{2}f_u-v_g\frac{\partial f_l}{\partial z}+\frac{1}{2}\tilde{\omega}_u''\frac{\partial^2 f_l}{\partial z^2}=0, \quad (90)$$
$$i\frac{\partial f_l}{\partial t}+\frac{\Delta}{2}f_l+v_g\frac{\partial f_u}{\partial z}+\frac{1}{2}\tilde{\omega}_l''\frac{\partial^2 f_u}{\partial z^2}=0.$$

Here we have set $v_g\equiv iv_{lu}$. The Bloch functions may be chosen to be purely real at the band gap; making this choice, v_{lu} is purely imaginary [cf. Eq. (38)], v_g is purely real, and $v_{ul}=iv_g$. Equation (90) shows how the two bands u and l are treated here in one class and the other bands in another: The interaction between the envelope functions associated with the bands u and l appears in a *dynamical* sense in that the functions must satisfy a set of coupled equations; the interaction with the remote bands resides in the effective-mass-type terms $\tilde{\omega}_{u,l}''$, simply modifying the evolution of the envelope functions through their curvature. Because of the closeness of the bands u and l, the first of these interactions is described in order η^1; the second is described in order η^2. If we are content to work to order η, the effects of the remote bands can be neglected and Eqs. (90) simplify to

$$i\frac{\partial f_u}{\partial t}-\frac{\Delta}{2}f_u-v_g\frac{\partial f_l}{\partial z}=0, \quad (91)$$
$$i\frac{\partial f_l}{\partial t}+\frac{\Delta}{2}f_l+v_g\frac{\partial f_u}{\partial z}=0.$$

We show in Sec. VII that Eqs. (91) can be rewritten in the form of the familiar coupled-mode equations. However, the usual derivation of those equations is only valid in the limit of a shallow grating [17]. Although Eqs. (91) lead to equations of the same form, they are valid for much stronger gratings, as long as all other bands are remote from the gap of interest. The coupling strength is determined for a deep grating by the parameters Δ and v_g, which must be evaluated from the actual Bloch functions at the gap.

B. Intensity index $s=1$: Nonlinear coupled-envelope-function equations

We now consider a nonlinearity characterized by an intensity index $s=1$; then it is only generally consistent to take the analysis to order η^1, as we have previously discussed. The only *linear* effect appearing to this order is the dynamical coupling between the envelope functions $f_u(z,t)$ and $f_l(z,t)$, as described by Eqs. (91). To include the nonlinear effects, note that to lowest order we have

$$A^{\pm}(z,t)=a[F_u^{(0)}\psi_u^{\pm}(z_0)+F_l^{(0)}\psi_l^{\pm}(z_0)]e^{-i\omega_0 t_0}+\text{c.c.} \quad (92)$$

[see Eqs. (80) and (81)]; so, using Eq. (21), we have

$$A^+(z,t)+A^-(z,t)=a\sqrt{n(z_0)}[F_u^{(0)}\phi_u(z_0) + F_l^{(0)}\phi_l(z_0)]e^{-i\omega_0 t_0}+\text{c.c.} \quad (93)$$

Then, using Eq. (44) for the components of **B**, we find

$$B^{\pm}(z,t)=-\frac{3}{2}n_0\omega_0 a^3|F_u^{(0)}\phi_u(z_0) + F_l^{(0)}\phi_l(z_0)|^2[F_u^{(0)}\phi_u(z_0) + F_l^{(0)}\phi_l(z_0)]\frac{\chi^{(3)}(z_0)}{\sqrt{n(z_0)}}e^{-i\omega_0 t_0}+\text{c.c.}, \quad (94)$$

where, as in Sec. V, we have neglected the effects of third-harmonic generation. With an assumed intensity index $s=1$, **B** leads to an additional term on the right-hand side of Eq. (84) [see Eq. (53)]. Putting that new equation into $\Psi_u^\dagger$ and then into $\Psi_l^\dagger$ we find, respectively

$$i\frac{\partial F_u^{(0)}}{\partial t_1}=\sigma_u F_u^{(0)}-iv_{ul}\frac{\partial F_l^{(0)}}{\partial z_1}+\frac{(\Psi_u^\dagger\cdot\hat{\mathbf{B}})e^{i\omega_0 t_0}}{\eta aN}, \quad (95)$$

$$i\frac{\partial F_l^{(0)}}{\partial t_1}=\sigma_l F_l^{(0)}-iv_{lu}\frac{\partial F_u^{(0)}}{\partial z_1}+\frac{(\Psi_l^\dagger\cdot\hat{\mathbf{B}})e^{i\omega_0 t_0}}{\eta aN}$$

rather than the simpler equations (87); here again $\hat{\mathbf{B}}$ is the positive-frequency part of **B**, with respect to t_0, this time in the approximation of Eq. (94).

Since we are only carrying the calculation to order η we can use

$$i\eta\frac{\partial}{\partial t_1}=i\frac{\partial}{\partial t}, \quad (96)$$

$$i\eta\frac{\partial}{\partial z_1}=i\frac{\partial}{\partial z}$$

for functions that do not depend on z_0 or t_0, rather than the more complicated equation (65). Then Eqs. (95) lead directly to the equations

$$i\frac{\partial f_u}{\partial t}-\frac{\Delta}{2}f_u-v_g\frac{\partial f_l}{\partial z}+\theta_u(z,t)=0, \quad (97)$$

$$i\frac{\partial f_l}{\partial t}+\frac{\Delta}{2}f_l+v_g\frac{\partial f_u}{\partial z}+\theta_l(z,t)=0,$$

where

$$\theta_{u,l}(z,t)=\frac{3}{2}n_0\omega_0\int_0^d\chi^{(3)}(\tilde{z})\phi_{u,l}^*(\tilde{z})|f_u(z,t)\phi_u(\tilde{z}) + f_l(z,t)\phi_l(\tilde{z})|^2[f_u(z,t)\phi_u(\tilde{z})+f_l(z,t)\phi_l(\tilde{z})]d\tilde{z} \quad (98)$$

and we have used the periodicity of $\chi^{(3)}(\tilde{z})$ and the $\phi_{u,l}(\tilde{z})$ to restrict the integral to a unit cell.

In Sec. V, where only one band is of dynamical importance in the way that both u and l are here, there is only one coefficient α [Eq. (76)] that describes how the sampling of the underlying $\chi^{(3)}(z_0)$ nonlinearity by the Bloch function $\phi_{mk}(z_0)$ leads to a modification of the dynamical equation that the envelope function $f_{mk}(z,t)$ satisfies. Here Eq. (98) spawns a number of different such coefficients, describing in detail how the sampling of the nonlinearity by the Bloch functions $\phi_{u,l}(z_0)$ leads to a modification in the self-interactions and mutual interactions of the associated envelope functions $f_{u,l}(z,t)$. Defining

$$\alpha_{pqrs}=\frac{3}{2}n_0\omega_0\int_0^d\chi^{(3)}(\tilde{z})\phi_p^*(\tilde{z})\phi_q(\tilde{z})\phi_r^*(\tilde{z})\phi_s(\tilde{z})d\tilde{z}, \quad (99)$$

expanding the $\theta_{u,l}(z,t)$, and gathering up the terms we find that Eqs. (97) become

$$i\frac{\partial f_u}{\partial t}-\frac{\Delta}{2}f_u-v_g\frac{\partial f_l}{\partial z}+\alpha_{uuuu}|f_u|^2f_u+\alpha_{ulll}|f_l|^2f_l + \alpha_{uull}(2|f_l|^2f_u+f_l^2f_u^*)+\alpha_{uuul}(2|f_u|^2f_l+f_u^2f_l^*)=0, \quad (100)$$

$$i\frac{\partial f_l}{\partial t}+\frac{\Delta}{2}f_l+v_g\frac{\partial f_u}{\partial z}+\alpha_{luuu}|f_u|^2f_u+\alpha_{llll}|f_l|^2f_l + \alpha_{lull}(2|f_l|^2f_u+f_l^2f_u^*)+\alpha_{luul}(2|f_u|^2f_l+f_u^2f_l^*)=0.$$

These equations are the central result of this section. Note that for a given band structure the α_{pqrs} must be determined from the Bloch functions and the distribution of the nonlinearity. We show in the next section that equations very similar to the usual nonlinear coupled-mode equations may be derived from Eqs. (100), but there are some new terms that appear. Recall that the standard derivation of the usual nonlinear coupled-mode equations relies on the weakness of the grating. We have not made such an assumption here; rather, we have only required that the other bands be remote from the two bands at the edges of the gap of interest. The new terms that appear are a consequence of the strength of the grating that the present formalism can describe and vanish in the conventional limit of a shallow grating.

We note that the effect of including a nonlinearity of intensity index $s=1$ and carrying the analysis to the order of η^1 has been to add to the simpler equations (91) that appear to that order in the absence of any nonlinearity a series of nonlinear terms. If instead a weaker nonlinearity of intensity index $s=2$ is present, the nonlinearity enters at the order of analysis (η^2) at which the dispersive contribution from the remote bands appear in the equations; it is easy to confirm the result that, to order η^2, the same series of nonlinear terms are added then to the more complicated equations (90) rather than to Eqs. (91).

VII. TRANSFORMATION TO STANDARD COUPLED-MODE FORM

Of the results derived until now, Eqs. (100) are different, and have not, as far as we know, been derived in other contexts [21]; in this section we therefore concentrate on these equations. First, note from definition (99) that Eqs. (100) contain five, rather than eight, independent nonlinear coeffi-

cients, since, for example, from Eq. (66) $\alpha_{ulll}=\alpha_{lull}$. In order to simplify the equation further we recall that we have assumed an expansion about $k=0$ or $k=\pi/d$. Since the group velocity at these positions vanishes, the Bloch functions are real and have a definite parity. We therefore immediately see from the definitions (99) that α_{ulll} and α_{luuu} vanish, so that only three independent nonlinear coefficients remain.

To cast Eqs. (100) in a more familiar form we introduce the envelope functions [25],

$$G_{\pm}=(f_u \mp i f_l)/2. \tag{101}$$

In terms of these functions, Eqs. (100) attain the form [21]

$$\begin{aligned}
&+i\frac{\partial G_+}{\partial z}+\frac{i}{v_g}\frac{\partial G_+}{\partial t}+\kappa G_-+\Gamma_0|G_+|^2G_+ ++2\Gamma_0|G_-|^2G_+\\
&\quad+\Gamma_1(|G_+|^2+|G_-|^2)G_-+\Gamma_1(G_+G_-^*+G_-G_+^*)G_+\\
&\quad+\Gamma_2G_+^2G_-^*=0,
\end{aligned} \tag{102}$$

$$\begin{aligned}
&-i\frac{\partial G_-}{\partial z}+\frac{i}{v_g}\frac{\partial G_-}{\partial t}+\kappa G_+ +\Gamma_0|G_-|^2G_- ++2\Gamma_0|G_+|^2G_-\\
&\quad+\Gamma_1(|G_+|^2+|G_-|^2)G_+ +\Gamma_1(G_+G_-^*+G_-G_+^*)G_-\\
&\quad+\Gamma_2G_-^2G_+^*=0,
\end{aligned}$$

where the linear coupling coefficient is given by

$$\kappa=\frac{\Delta}{2v_g}, \tag{103}$$

where v_g is defined below Eq. (90), and the nonlinear coefficients

$$\begin{aligned}
\Gamma_0&=\frac{1}{8v_g}(\alpha_{uuuu}+2\alpha_{uull}+\alpha_{llll}),\\
\Gamma_1&=\frac{1}{8v_g}(-\alpha_{uuuu}+\alpha_{llll}),\\
\Gamma_2&=\frac{1}{8v_g}(\alpha_{uuuu}-6\alpha_{uull}+\alpha_{llll}).
\end{aligned} \tag{104}$$

Equations (102) are similar to the usual coupled-mode equation for shallow gratings [4]. However, note some important differences. The first of these is that the terms in Eqs. (102) have coefficients different from the equivalent terms in Ref. [4]. As an example, in Eq. (102) the coupling coefficient κ is given in terms of the exact eigenvalues and eigenfunctions of the linear system [Eq. (103)]. In contrast, the coupling coeffient for Mth-order Bragg reflection for shallow gratings is $\kappa=\pi\Delta n/\lambda$, where Δn is the Mth Fourier amplitude of the refractive index [4]. But the most obvious difference between Eqs. (102) and the standard nonlinear coupled-mode equations [4] is that in the latter the nonlinear terms with Γ_1 and Γ_2 do not appear.

To show that our results reduce in the appropriate way in the shallow grating limit, recall that in this limit the Bloch functions at the center and at the edges of the Brillouin zone can simply be written as

$$\cos(M\pi z/d), \quad \sin(M\pi z/d), \tag{105}$$

where the positive integer M indicates the Bragg order; M is odd at the Brillouin zone edge, while M is even at the center. Though the normalization has not been given explicitly, it is sufficient to note that all Bloch functions have identical normalization prefactors. It is then easy to see that for shallow gratings and for a uniform nonlinearity $\alpha_{uuuu}=\alpha_{llll}=3\alpha_{uull}$. From Eqs. (104) we thus find that in this limiting case $\Gamma_1=\Gamma_2=0$, as required. Note more generally that for shallow gratings the nonlinear coefficients are related to the lowest Fourier components of the nonlinearity; indicating the nth Fourier component of $\chi^{(3)}(z)$ by $\chi_n^{(3)}$ we find

$$\Gamma_0\propto\chi_0^{(3)}, \quad \Gamma_1\propto\chi_1^{(3)}, \quad \Gamma_2\propto-\chi_2^{(3)}, \tag{106}$$

all with the same precoefficient. This result was obtained by assuming that the nonlinearity has the same phase as the refractive index distribution. This result helps explain the significance of the nonlinear terms in Eqs. (102). The self- and cross-phase modulation terms, proportional to Γ_0, are well known and lead to a nonlinear shift in the Bragg condition. The first terms proportional to Γ_1 correspond to a nonlinear change in the grating depth [21]; as expected, this contribution depends only on the first Fourier component of $\chi^{(3)}$, which varies at the same rate as the grating. The second terms proportional to Γ_1 in Eqs. (102) express the nonlinear shift of the Bragg resonance due to the first Fourier component of the electric-field density. Finally, as expected, the phase conjugation terms proportional to Γ_2 rely on the next higher Fourier component of the nonlinearity of the nonlinear refractive index.

Because of definition (99) the three coefficients α are not independent of each other. In fact, using the method described in Ref. [26] it is easy to show that

$$\alpha_{uuuu}\alpha_{llll}>\alpha_{uull}^2, \tag{107}$$

under the assumption that the nonlinearity has the same sign everywhere. The equality in (107) can be ruled out as it would occur if $\phi_l^2=\phi_u^2$ which is not true as they are different eigenfunctions of a Sturm-Liouville equation. From inequality (107) it can easily be shown that also

$$\alpha_{uuuu}+\alpha_{llll}>2\alpha_{uull}, \tag{108}$$

so that, in terms of the Γ coefficients [Eq. (104)],

$$|\Gamma_0|>|\Gamma_1|,|\Gamma_2|. \tag{109}$$

To finish this section we illustrate some of the properties of the Bloch functions and we discuss the transformation (101). Figure 2 shows the Bloch functions for a periodic structure consisting of GaAs ($n=3.59$) and a polymer ($n=1.5$). The period $d=1$, the thickness of the GaAs layers is $d_{\mathrm{GaAs}}=0.25$, and $d_{\mathrm{polymer}}=0.75$. The solid line represents ϕ_l, the Bloch function at the bottom of the lowest photonic band gap, while the dashed line is ϕ_u, that at the top of the gap. As required for Bloch functions at the Brillouin zone edge, both are real and have the required translational symmetry $\phi(z+d)=-\phi(z)$. Further, though they are similar to

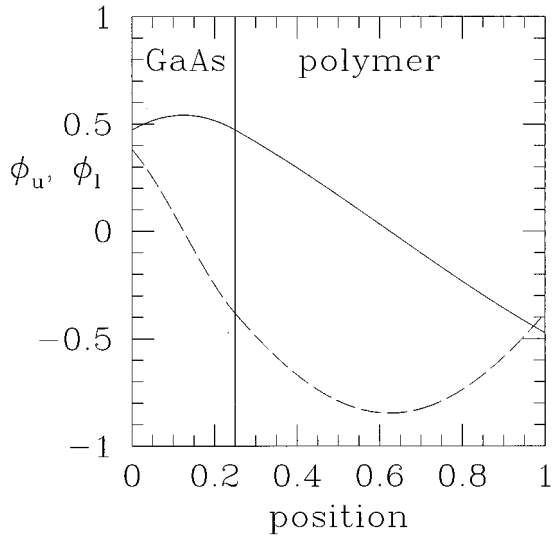

FIG. 2. Example of a Bloch function at the top (ϕ_u, dashed line) and bottom (ϕ_l, solid line) of the lowest photonic band gap as a function of the relative position in the grating period, for a structure with parameters given in the text.

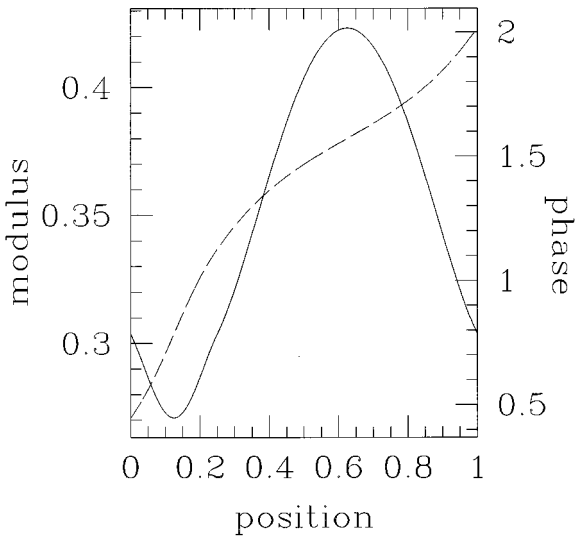

FIG. 3. Example of a pseudo plane wave as a function of relative position in the grating period, for a structure with parameters given in the text. The solid line is the modulus (left-hand scale), while the dashed line is the phase (right-hand scale).

the Bloch functions for a shallow grating [Eq. (105) with $M=1$], the details are clearly different. They also have the required properties that they have a definite parity and that the associated energy densities peak in the correct media: ϕ_l^2 peaks in the high-index medium, while ϕ_u^2 peaks in the low-index medium.

As mentioned, in the final expression of the coupled-mode equations [Eqs. (102)] the envelope functions $G_\pm$ are linear combinations of the envelope functions $f_{l,u}$ that multiply the Bloch functions in expression (80) for the electromagnetic field [see Eq. (101)]. Clearly, in the shallow grating limit Eq. (101) corresponds to transforming the underlying basis functions that multiply the envelope functions, from the simple trigonometric functions in (105) to plane waves with wave numbers $\pm M\pi/d$. More generally, the transformation (101) can be interpreted as introducing a *pseudo-plane-wave* basis, i.e., plane waves with higher-order harmonics introduced by the deep grating [21]. As an example, the pseudo plane wave following from the Bloch functions in Fig. 2 is given in Fig. 3. The solid line in Fig. 3 is the modulus of the pseudo plane wave (left-hand scale), while the dashed line gives its phase (right-hand scale). Clearly Fig. 3 does not represent a plane wave since the modulus is not constant and the phase does not progress linearly. Note also that the deviations in Fig. 3 occur on the scale of a single period and can never be captured by a change in the envelope functions, which vary on a much longer length scale. Finally, note that the phase of the pseudo plane wave increases by π over a single period, as required at the Brillouin zone edge.

VIII. COUPLED-MODE COEFFICIENTS FOR DEEP GRATINGS

In this section we evaluate the coefficients in our coupled-mode equations (102) for a few different cases. We first consider the linear properties these equations predict; in particular, we look at the positions of the upper and lower edges of the lowest photonic band gap. These are directly related to the optical frequency ω_0 at the center of the gap [Eq. (80)] and the width of the gap, which determines the coupling coefficient κ by Eq. (103). Shown in Fig. 4 are the frequencies of the upper and lower edges of the lowest photonic band gap in a periodic structure consisting of uniform layers of GaAs and AlAs in units of c/d. The GaAs layers have thickness d_{GaAs} and refractive index $n_{\mathrm{GaAs}}=3.59$, while the AlAs layers have thickness d_{AlAs} and refractive index $n_{\mathrm{AlAs}}=2.98$. The positions are shown as a function of the GaAs filling fraction d_{GaAs}/d, where $d=d_{\mathrm{GaAs}}+d_{\mathrm{AlAs}}$. The

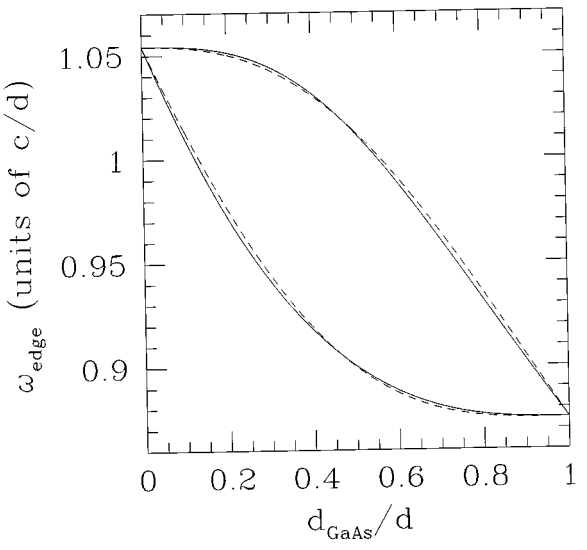

FIG. 4. Exact positions (solid lines) and positions according to the shallow grating approximation (dashed lines) of the band edges of a periodic GaAs-AlAs structure with refractive indices 3.59 and 2.98, respectively. The structure has a period d and the GaAs and AlAs layers have thicknesses d_{GaAs} and d_{AlAs}, respectively.

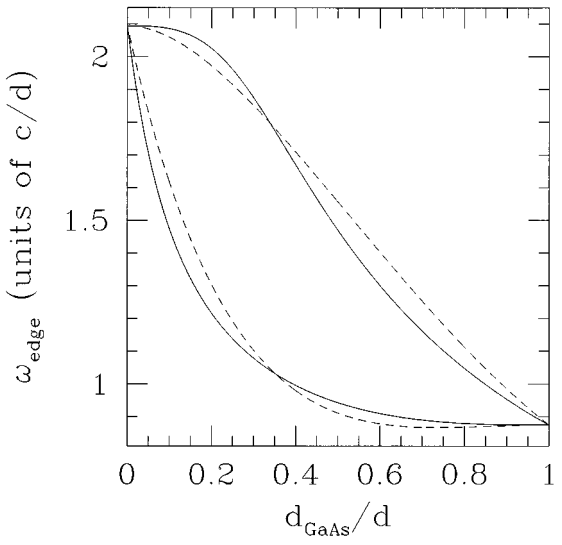

FIG. 5. Similar to Fig. 4 but for GaAs and a polymer with a refractive index of 1.5.

solid lines show the exact positions of the band gap edges, while the dashed line shows the results assuming the structure is shallow. Recall that Eqs. (102) make use of the exact positions of the photonic band-gap edges. Clearly, the assumption that the grating is shallow leads to results that are incorrect. Though the error in Fig. 4 may not seem very large, it is important to note that the deviations can be a noticeable fraction of the gap width. The grating properties change drastically around the band edges and it is thus important to correctly calculate their positions. Figure 5 is similar to Fig. 4, but for a periodic structure consisting of layers of GaAs and polymer ($n=1.5$). As expected, the errors introduced by the shallow grating approximation are more severe in this case of larger refractive index contrast.

Turning now to the nonlinear Γ coefficients, recall that in the limit in which the grating is shallow and the nonlinearity is uniform we find that $\Gamma_1=\Gamma_2=0$. As a comparison we show in Fig. 6 the Γ coefficients [in units of $c\chi^{(3)}/dv_g$ and with $n_0=1$] for a GaAs-AlAs system, as a function of the GaAs filling fraction. In the figure the solid line indicates Γ_0, the short-dashed line Γ_1, and the long-dashed line is Γ_2. As expected, for $d_{GaAs}/d\rightarrow 0,1$ we see that $\Gamma_{1,2}\approx 0$ as the usual shallow grating results must then be obtained. More generally, while Γ_1 and Γ_2 are certainly smaller than Γ_0, $\Gamma_1\approx 0.16\Gamma_0$ at $d_{GaAs}/d=0.44$. Note also that for AlAs Γ_0 is more than twice as large as for GaAs; this is due to the normalization of the Bloch functions [Eq. (20)]. Finally, in Fig. 7 we show similar results, but for a periodic GaAs-polymer structure with refractive indices as above and assuming the nonlinearity in the polymer to vanish. Clearly, as $d_{GaAs}/d\rightarrow 0$ the structure is linear and all nonlinear coefficients must vanish. Further, as $d_{GaAs}/d\rightarrow 1$, $\Gamma_{1,2}=0$ since the grating is then shallow and the nonlinearity is uniform. However, in the intermediate cases the new nonlinear coefficients Γ_1 and Γ_2 can be as large Γ_0 [while still satisfying inequality (109)]; in such a case, therefore, use of our approach is crucial.

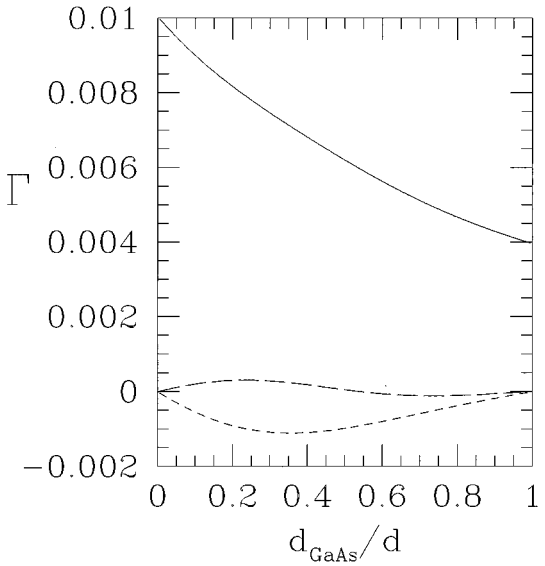

FIG. 6. Nonlinear coefficients Γ (solid line), Γ_1 (long-dashed line), and Γ_2 (short-dashed line) for a GaAs-AlAs structure with refractive indices 3.59 and 2.98, respectively, in units of $c\chi^{(3)}/dv_g$ and with $n_0=1$.

IX. SOLUTIONS TO THE COUPLED-MODE EQUATIONS FOR DEEP GRATINGS

In this section we discuss some of the solitary-wave solutions to the coupled-mode equations for deep gratings (102), both for finite (Secs. IX A and IX B) and also for infinite (Secs. IX C and IX D) geometries. In doing so we point out differences with the solutions to the conventional coupled-mode equations for shallow gratings. We note that the solutions described in Sec. IX C are generalizations of those

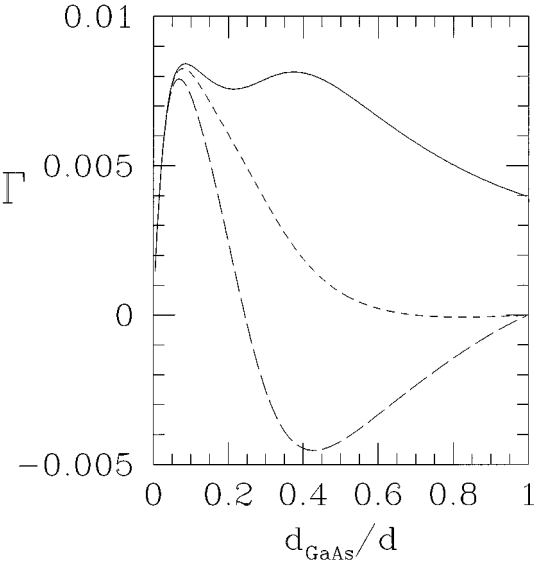

FIG. 7. Nonlinear coefficients Γ (solid line), Γ_1 (long-dashed line), and Γ_2 (short-dashed line) for a GaAs-polymer structure with refractive indices 3.59 and 1.5, respectively, and a vanishing nonlinearity in the polymer, in units of $c\chi^{(3)}_{GaAs}/(dv_g)$, and with $n_0=1$.

found in the experiments of Eggleton *et al* [13].

As a general point we mention that, while the coupled-mode equations for shallow gratings (for which $\Gamma_1=\Gamma_2=0$) have well-known bright and dark solutions [7,27], to our knowledge Eqs. (102) have not been studied previously. We will see that the soliton solution of Eqs. (102) can differ qualitatively from those of the equations valid for shallow gratings. We use two different approaches. The first of these is a variation on that of Feng and Kneubühl [7] and makes use of Stokes parameters. The second is the method described by Kivshar and Flytzanis [27] and allows us to find closed-form stationary solutions in the stationary limit. In discussing the solutions to Eqs. (102) we emphasize the influence of the extra nonlinear coefficients on the shape of the solutions.

A. Solutions to the linearized coupled-mode equations

Recall that while the linear equations have exactly the same form for shallow and for deep gratings, the coefficients have different values (see Figs. 4 and 5). Though these differences may sometimes seem modest, we emphasize that the properties of periodic structures near a Bragg resonance vary rapidly as a function of wavelength. A small error in the position of the edges of the photonic band gap, say, can thus lead to large errors. This was discussed earlier in Ref. [21].

Another key point in solving the present coupled-mode equations on a finite interval is the application of the boundary conditions at the interfaces with the outside media. Recall that in conventional coupled-mode theory the fields are expanded in forward and backward propagating modes; since these are also the eigenmodes of uniform media, matching the fields across the interfaces is straightforward. This is even true if the average refractive index in the grating differs from the refractive indices of the outside media, leading to Fresnel reflections at the interfaces. The reason the application of the boundary conditions for deep gratings is more complicated is our expansion of the fields in terms of pseudo plane waves (see Fig. 3), which must be matched to plane waves in the outside media. This depends on the details of the Bloch functions, which must therefore be calculated explicitly, even though this is not necessary to solve the coupled mode equations [Eqs. (102)].

B. Stationary solutions on a finite interval

It is well known that nonlinear grating structures of finite extent can exhibit bistability [1]. This is a particularly interesting case to consider as the nonlinear wave equation, which is now an ordinary differential equation, can easily be solved for this case, allowing a comparison with the results from our approximate theory.

While the harmonically varying solutions of the conventional coupled-mode equations on a finite interval can be found in terms of Jacobi elliptic functions [1], finding an analytic solution appears to be impossible for the present coupled-mode equations (102). Though, of course, the resulting ordinary differential equations can be straightforwardly integrated numerically, as noted above the application of the boundary conditions requires knowledge of the details of the Bloch functions (Fig. 2) of the periodic structure. However, once they are known, this can be implemented in a simple fashion.

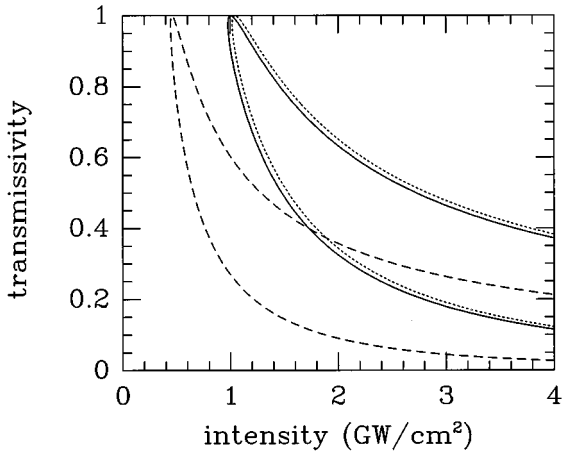

FIG. 8. Transmissivity as a function of incident intensity for a GaAs-AlAs thin-film stack. The stack consists of 200 periods, each consisting of 125-nm GaAs ($n=3.59$) and AlAs ($n=2.98$) layers, while $\lambda=1.5522\mu$ m. Shown are the results of exact calculations (solid line), standard coupled-mode theory (short-dashed line), and Eqs. (102) (long-dashed line).

Figure 8 gives the results of three types of calculations for a periodic structure with parameters given in the caption: exact results, following from a full solution of Maxwell's equations (solid line), results from Eq. (102) (short-dashed line), and results from standard coupled-mode theory (long-dashed line). Clearly, the results of our deep grating theory are close to the exact results and are superior to those from standard coupled-mode theory. We note in passing that all three methods indicate the existence of a low-transmissivity branch, which, on the present scale, coincides with the horizontal axis. At high intensities this branch folds back and links up with the branches shown in Fig. 8. Full time-dependent simulations of the same problem have indicated that not all solutions in Fig. 8 are stable [28,29], but such behavior can of course not be ascertained within the limitation of harmonically varying fields.

C. Solitary-wave solutions using Stokes parameters

We next consider solitary-wave solutions to Eqs. (102) on an unbounded interval. To do so, following previous work [7] we look for solutions of the form

$$G_{\pm}(z,t)=B_{\pm}(z-vt)e^{-iv_g\delta t}\equiv B_{\pm}(x)e^{-iv_g\delta t}, \quad (110)$$

where δ is a detuning. The ansatz (110) turns Eqs. (102) into a set of two coupled ordinary complex differential equations. Defining then the (real) Stokes parameters through

$$S_i=\mathbf{B}^{\dagger}\sigma_i\mathbf{B}, \quad (111)$$

where the σ_i are the Pauli matrices and $\mathbf{B}$ is the column vector with elements (B_+,B_-), it is easy to find the four real equations for the Stokes parameters

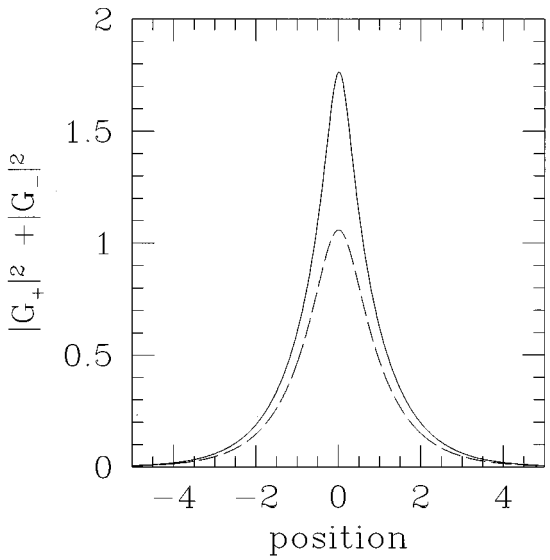

FIG. 9. Example of a soliton solution for a deep nonlinear periodic structure with $\kappa=1$, $v=0.5$, and $\delta=0$, while the units of field strength have been chosen such that $\alpha_{uuuu}=2.1$, $\alpha_{uull}=1.9$, and $\alpha_{llll}=2.1$, so that $\Gamma=1$, $\Gamma_1=0$, and $\Gamma_2=-0.9$. Shown as a function of position is $|G_+|^2+|G_-|^2$, which is proportional to the energy density (solid line). As a comparison, also shown is the solution for the case in which deep grating effects are ignored, i.e., $\Gamma=1$ and $\Gamma_1=\Gamma_2=0$, while the other parameters are unchanged (dashed line).

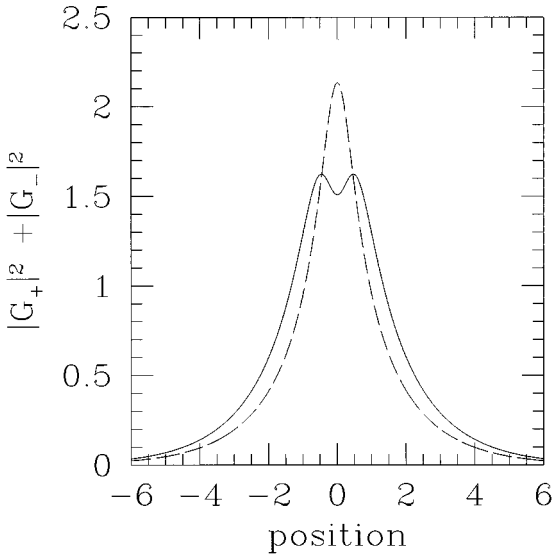

FIG. 10. Example of a soliton solution for nonlinear periodic structure with $\kappa=1$, $v=0$, and $\delta=-1/2\sqrt{2}$, while the units of field strength have been chosen such that $\alpha_{uuuu}=6$, $\alpha_{uull}=0.25$, and $\alpha_{llll}=1.5$, so that $\Gamma=1$, $\Gamma_1=-0.5625$, and $\Gamma_2=0.75$. Shown as a function of position is $|G_+|^2+|G_-|^2$, which is proportional to the energy density. As a comparison, also shown is the solution for the case in which deep grating effects are ignored, i.e., $\Gamma=1$ and $\Gamma_1=\Gamma_2=0$, while the other parameters are unchanged (dashed line).

$$S_0'=-2\kappa S_2-2\Gamma_1 S_0S_2-2\Gamma_2 S_1S_2,$$

$$S_1'=2\delta S_2+3\Gamma S_0S_2-v\Gamma S_3S_2+2\Gamma_1 S_1S_2-\Gamma_2 S_0S_2+v\Gamma_2 S_3S_2,$$

$$S_2'=-2\kappa S_0+2v\kappa S_3-2\delta S_1-3\Gamma S_0S_1+v\Gamma S_3S_1-2\Gamma_1 S_0^2+2v\Gamma_1 S_0S_3-2\Gamma_1 S_1^2-\Gamma_2 S_0S_1+v\Gamma_2 S_3S_1, \tag{112}$$

$$S_3'=vS_0',$$

where the prime indicates differentiation with respect to x. It is straightforward but tedious to demonstrate that this system has three conserved quantities, namely,

$$S_0^2-S_1^2-S_2^2-S_3^2=0,$$

$$S_3-vS_0, \tag{113}$$

$$\kappa S_1+\delta S_0+\frac{3}{4}\Gamma S_0^2-\frac{1}{4}\Gamma S_3^2+\Gamma_1 S_0S_1+\frac{1}{4}\Gamma_2(S_1^2-S_2^2).$$

The first of these follows from the definition of the Stokes parameters and is a consequence of the fact that absolute phase is unimportant here. While the system (112) with conserved quantities (113) is now, in principle, reduced to quadrature, the conserved quantities are sufficiently complicated to prevent us finding the relevant integral in closed form. We therefore consider a special case. We concentrate on bright solutions for which the fields vanish as $|x|\to\infty$, though we show below that Eqs. (102) also possess other solutions.

We note that Eqs. (112) have solutions for which S_0, S_1, and S_3 are even functions, while S_2 is odd, and these are the solutions we are considering here. These parity properties then imply that we can define a ''center,'' which we take to be at $x=0$. Here we consider the S_i at $x=0$ for the solutions of Eqs. (112); this is not only of interest in its own right, but also provides convenient initial conditions when solving Eqs. (102) or (112) numerically.

Since we are considering solutions for which S_2 is odd, it must vanish at the center. We also note that for bright solutions, for which the field envelopes must vanish at $x\to\pm\infty$, the second and third conserved quantities in Eqs. (113) vanish. Now from the first and second of the conserved quantities (113) we then find that

$$S_1=\pm S_0/\gamma,$$

$$S_0=\frac{4\gamma(\kappa-\delta\gamma)}{(2\gamma^2+1)\Gamma-4\gamma\Gamma_1+\Gamma_2}, \tag{114}$$

$$S_3=vS_0,$$

where

$$\gamma=1/\sqrt{1-v^2} \tag{115}$$

is the Lorentz factor and the negative sign in the first of Eqs. (114) is found to apply. By Eqs. (114) all Stokes parameters are thus known; this provides a convenient starting point for

finding the solitary-wave solutions numerically. Note that, although by definition S_0 is a positive quantity, the right-hand side of the second of Eqs. (114) can be negative, especially when Γ_1 is sufficiently large. Such solutions, which are not prevented by inequality (109), must be disregarded.

Since all Stokes parameters are known, the system (112) can also be used to evaluate higher derivatives. In particular, it can be shown that S_0'' can be either positive or negative. In the latter case the solution would be expected to be singly peaked, while in the former case it must exhibit auxiliary peaks for it to vanish as $x \to \pm\infty$. Examples of both types of solutions are shown in Figs. 9 and 10. In both figures the solid lines represent solutions to the full coupled-mode equations (102), while the dashed lines represent the associated solutions for shallow gratings, obtained by ignoring the nonlinear terms proportional to Γ_1 and Γ_2. We note that the double-peaked solution in Fig. 10 is typical for deep gratings and does not occur in shallow gratings, for which the solutions [5] are always single peaked. We note in passing that the new solutions shown in Figs. 9 and 10 can be considered to be generalization of the grating solitons observed by Eggleton *et al.* [13] in a shallow grating.

D. Stationary solitary-wave solutions

Another limit in which exact results can be obtained is when $v=0$, i.e., when the solitary wave is stationary. These solutions can be found using a number of different methods, including that of Kivshar and Flytzanis [27], who applied it to the closely related problem of nonlinear discrete lattices. It is their approach we use here. To start we use Eqs. (100), which, of course, are fully equivalent to the coupled-mode equations (102). We set

$$f_{l,u}(z,t) = g_{1,2}(z) e^{-i\delta t} \tag{116}$$

and take the $g_{1,2}$ to be *real*. This implies that the envelope functions $G_{\pm}$ [see Eq. (101)] are each other's complex conjugate, as is the case for the stationary solitary-wave solutions to the shallow gratings. This substitution leads to the equations

$$\begin{aligned} g_1' &= -\Delta_2 g_2 + \alpha_1 g_2^3 + 3\alpha_2 g_1^2 g_2, \\ g_2' &= +\Delta_1 g_1 - \alpha_3 g_1^3 - 3\alpha_2 g_2^2 g_1, \end{aligned} \tag{117}$$

for convenience, we have set $\alpha_1 = \alpha_{uuuu}$, $\alpha_2 = \alpha_{uull}$, and $\alpha_3 = \alpha_{llll}$. Further,

$$\Delta_1 = -\Delta/2 - \delta, \quad \Delta_2 = \Delta/2 - \delta, \tag{118}$$

and the prime indicates differentiation with respect to z/v_g. Note from definitions (118) that at the top of the photonic band gap ($\delta = \Delta/2$) we have $\Delta_1 = -\Delta$ and $\Delta_2 = 0$, while at the bottom $\Delta_1 = 0$ and $\Delta_2 = \Delta$. Equations (117) are very similar to those of Kivshar and Flytzanis [27], but have more complicated nonlinear terms. It is easy to see that Eqs. (117) form a Hamiltonian system with $g_{1,2}$ playing the roles of q and p, respectively, and with

$$\mathcal{H} = -\frac{1}{2}(\Delta_1 g_1^2 + \Delta_2 g_2^2) + \frac{1}{4}(\alpha_3 g_1^4 + 6\alpha_2 g_1^2 g_2^2 + \alpha_1 g_2^4). \tag{119}$$

Now each orbit of this Hamiltonian corresponds to a solution pair (g_1, g_2). However, the solitary-wave solutions, i.e., solutions that settle to definite values as $z \to \infty$, correspond to the separatrices. We must therefore identify the fixed points of the system (117) and the orbits connecting the saddle points. Orbits starting and finishing at the origin in (g_1, g_2) space correspond to bright solitary waves, while others correspond to dark and gray solitary waves and to bright solutions on a pedestal [27].

Below we discuss some of these solutions. In doing so we assume that the nonlinearity is positive and thus $\alpha_{1,2,3} > 0$. It is easy to see that for negative nonlinearities the solutions are very similar. If the spatial distribution of the nonlinearity is chosen such that not all nonlinear coefficients α_i have the same sign, then an entirely new class of solutions becomes possible, but we do not cover these here. In discussing the solutions we identify three different regimes [27]. The first of these is defined by $\delta > \Delta/2$; here the frequency is *above* the photonic band gap. Since $\Delta_{1,2} < 0$ in this regime we find that the origin is the only fixed point and that it is a stable center. For this reason there are no solitary-wave solutions.

We next consider frequencies such that $-\Delta/2 < \delta < \Delta/2$, i.e., frequencies within the photonic band gap. Now $\Delta_1 < 0$, while $\Delta_2 > 0$; the system of equations (117) has a saddle at the origin and two stable centers at $g_1 = 0$ and $g_2 = \pm\sqrt{\alpha_1/\Delta_2}$. The only type of solution corresponds to the separatrix connecting the origin with itself, corresponding to a bright solitary wave. To find these solutions explicitly we define, following the analysis of Kivshar and Flytzanis [27], the ratio $r \equiv g_1/g_2$, which can be shown to satisfy

$$r' = (\Delta_2 + \Delta_1 r^2)^2 + 4E(\alpha_1 + 6\alpha_2 r^2 + \alpha_3 r^4), \tag{120}$$

where E is the value of the ''energy'' corresponding to the particular orbit associated with Hamiltonian $\mathcal{H}$ [Eq. (119)]; for the case we are considering here $E=0$ since the orbits include the origin. Equation (120) is now seen to yield

$$r = \sqrt{-\Delta_2/\Delta_1}\tanh(\sqrt{-\Delta_1\Delta_2}\, z/v_g) \equiv \sqrt{-\Delta_2/\Delta_1}\tanh(Cz). \tag{121}$$

Finally, then, the solutions for $g_{1,2}$ are found to be

$$\begin{aligned} g_1 &= \left[\frac{-2\Delta_1\Delta_2^2}{\alpha_1\Delta_1^2\cosh^4(Cz) - 6\alpha_2\Delta_1\Delta_2\cosh^2(Cz)\sinh^2(Cz) + \alpha_3\Delta_2^2\sinh^4(Cz)}\right]^{1/2}\sinh(Cz), \\ g_2 &= \left[\frac{2\Delta_2\Delta_1^2}{\alpha_1\Delta_1^2\cosh^4(Cz) - 6\alpha_2\Delta_1\Delta_2\cosh^2(Cz)\sinh^2(Cz) + \alpha_3\Delta_2^2\sinh^4(Cz)}\right]^{1/2}\cosh(Cz), \end{aligned} \tag{122}$$

where C was defined in Eq. (121). Using Eqs. (116) and (101), solutions to Eqs. (102) can then be found. It is interesting to note that in the shallow grating limit, in which $\alpha_1=\alpha_3=3\alpha_2$ [see the discussion below Eq. (105)], the denominators in Eqs. (122) can be factored into a perfect square, so that simple expressions for $g_{1,2}$ result; these are identical to those of Aceves and Wabnitz [5] and Feng and Kneubühl [7]. However, as shown in Sec. IX C, the solutions (122) can be qualitatively different from the associated shallow grating solutions (see Fig. 10).

We now finally turn to the third regime, where $\delta<-\Delta/2$; here the frequency is below the bottom of the photonic band gap, so that $\Delta_{1,2}>0$. There is now a larger number of critical points, the character of which depends on the relative sizes of the nonlinear coefficients α_i and on the detuning. However, for values of δ just below the photonic band gap there are two types of dark solutions, independent of the details of the α parameters, which are similar to those for shallow gratings (cf. Refs. [7] and [27]). Using a method similar to that described above, they can be found to be

$$g_2=\sqrt{\frac{(\Delta_2+\Delta_1 r^2)\pm r'}{\alpha_1+6\alpha_2 r^2+\alpha_3 r^4}},$$

$$g_1=r g_2, \tag{123}$$

where

$$r=\sqrt{\frac{\Delta_2^2-\alpha_1\Delta_1^2/\alpha_3}{2\Delta_1(\Delta_2-3\alpha_2\Delta_1/\alpha_3)}}\times\sinh[\sqrt{2\Delta_1(\Delta_2-3\alpha_2\Delta_1/\alpha_3)}z/v_g]. \tag{124}$$

It was shown in Refs. [27] and [7] that these solutions represent dark solitary waves (where the minus sign applies) in Eq. (123) and bright solitary waves on a pedestal (where the plus sign applies). These two types of solutions correspond to the large, ovoid orbits in Fig. 11. The existence of such solutions was also pointed out in Ref. [6].

Recall that for detunings δ well below the photonic band gap of deep gratings other critical points, with associated solitary-wave solutions, can appear; these have no equivalent in shallow gratings. The positions of these critical points are summarized in Table I. The critical points labeled as type I, II, and III occur also in shallow gratings with uniform nonlinearity, while type IV is different. This can be seen from Table I by realizing that if the grating is shallow and the nonlinearity is uniform then $\alpha_1\alpha_3=9\alpha_2^2$, shifting the type-IV critical points to infinity. Of course, the type-IV critical points exist only for detunings such that g_1 and g_2 are real.

As mentioned, the critical point at the origin (type I) is always a center for frequencies below the photonic band gap. The nature of the other critical points depends on the detuning and on the nonlinear α coefficients. Details can be found in Table II. The frequency dependence is associated with pitchfork bifurcations, which, depending on the relative values of the α_i, may occur for frequencies such that $\Delta_1/\Delta_2=3\alpha_2/\alpha_1$ and $\Delta_1/\Delta_2=\alpha_3/(3\alpha_2)$ (see Table II). Rather than discussing the ensuing solitary-wave solutions in detail, here we just sketch the types of orbits in the

TABLE I. Overview of positions of critical points for $\delta<-\Delta/2$, i.e., frequencies below the bottom of the photonic bad gap. The critical points of course exist only if g_1 and g_2 are real.

Type	g_1	g_2
I	0	0
II	0	$\pm\sqrt{\Delta_2/\alpha_1}$
III	$\pm\sqrt{\Delta_1/\alpha_3}$	0
IV	$\pm\sqrt{\frac{\alpha_1\delta_1-3\alpha_2\Delta_2}{\alpha_1\alpha_3-9\alpha_2^2}}$	$\pm\sqrt{\frac{\alpha_3\delta_2-3\alpha_2\Delta_1}{\alpha_1\alpha_3-9\alpha_2^2}}$

(g_1,g_2) plane, from which the qualitative features of the solutions can then be learned. There are essentially two types of sets of solutions. Some typical examples are shown Figs. 11 and 12, while conditions for their existence are indicated in Table II. The orbits in Fig. 11 correspond to three different types of solitary-wave solutions. The small, butterfly-shaped orbits are unique to deep gratings, while the larger, ovoid orbits are very similar to the solitary-wave solutions found by Kivshar and Flytzanis [27]. The orbits in Fig. 12 correspond to four different types of solutions, all of which are unique to deep gratings. Though it is certainly possible to find explicit expressions for these solutions, we do not give them here.

X. DISCUSSION AND CONCLUSIONS

We have presented a systematic approach to obtaining the envelope-function equations for periodic media. Since it is based upon the Bloch functions of the structure, it is valid for

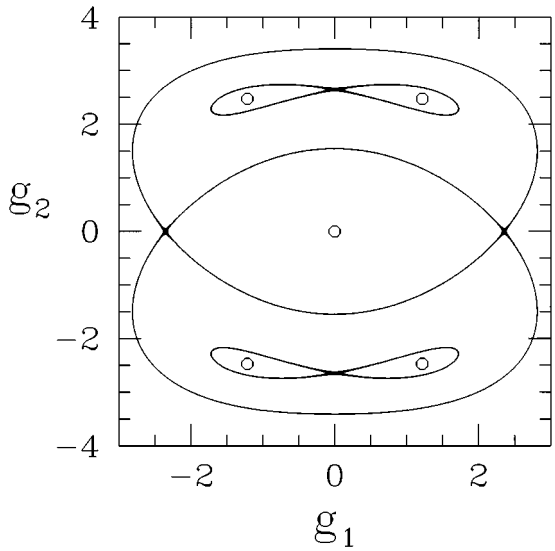

FIG. 11. Separatrices in the (g_1,g_2) plane, corresponding to stationary solutions to the coupled-mode equations. The particular parameters are $\kappa=1$ and $\delta=-6$, while the units of field strength have been chosen such that $\alpha_1=1.0$ and $\alpha_2=0.2$, $\alpha_3=0.9$. Two types of orbits are shown, corresponding to $E=-6.94$ (large, ovoid orbits) and $E=-12.25$ (small, butterflylike orbits), where E is the ''energy'' corresponding to the orbit according to Hamiltonian (119). While the saddle points can be clearly seen, the circles correspond to the positions of the centers.

TABLE II. Overview of types of the critical points for $\delta<-\Delta/2$, i.e., frequencies below the photonic band gap; note that the origin (type I) is always a center for these frequencies. The explicit frequency dependence enters through the ratio $\rho\equiv\Delta_1/\Delta_2$. The entries NA indicate that type-IV critical points do not exist if $\alpha_1<3\alpha_2<\alpha_3$. The last column gives the types of separatrices these new critial points give rise to and refers to Figs. 11 and 12. As discussed in the text, these correspond to stationary solitary-wave solutions to the coupled-mode equations. The entry 90° refers to a rotation over 90° of the orbits in the figure.

Condition 1	Condition 2	Type II	Type III	Type IV	Orbit
$\alpha_1,\alpha_3<3\alpha_2$	$\alpha_1\alpha_3<9\alpha_2^2$	center	$\rho<\alpha_3/3\alpha_2$: saddle $\rho>\alpha_3/3\alpha_2$: center	saddle	Fig. 12
$\alpha_1,\alpha_3>3\alpha_2$	$\alpha_1\alpha_3>9\alpha_2^2$	$\rho<3\alpha_2/\alpha_1$: center $\rho>3\alpha_2/\alpha_1$: saddle	saddle	center	Fig. 11
$\alpha_1<3\alpha_2<\alpha_3$		center	saddle	NA	NA
$\alpha_3<3\alpha_2<\alpha_1$	$\alpha_1\alpha_3<9\alpha_2^2$	$\rho<3\alpha_2/\alpha_1$: center $\rho>3\alpha_2/\alpha_1$: saddle	$\rho<\alpha_3/3\alpha_2$: saddle $\rho<\alpha_3/3\alpha_2$: center	saddle	Fig. 12
$\alpha_3<3\alpha_2<\alpha_1$	$\alpha_1\alpha_3>9\alpha_2^2$	$\rho<3\alpha_2/\alpha_1$: center $\rho>3\alpha_2/\alpha_1$: saddle	$\rho<\alpha_3/3\alpha_2$: saddle $\rho>\alpha_3/3\alpha_2$: center	center	Fig. 11 (90°)

shallow as well as deep gratings and also properly treats gratings with a nonuniform nonlinearity. While the envelope-function equations for shallow gratings can easily be derived heuristically, it is known that this method is internally inconsistent and arrives at the correct answer somewhat fortuitously [17]. In contrast, the method described in the present paper is systematic and thus so are the results obtained using it. While, as mentioned, the recent experimental results of Eggleton *et al.* [13] can be described by conventional coupled-mode theory, extensions of such experiments to material systems allowing for deeper gratings may require the more complete theory decribed here.

The many results presented in this paper are valid for different regimes, which depend on the relative importance of the nonlinearity and the dispersion and also on the amount of detail of the photonic dispersion curve that is required. The latter is determined mostly by the spectral width of the source; the wider the spectrum, the more details required. Though many of our results have been derived earlier, our systematic approach makes it clear under what conditions the various final results are to be used. This is somewhat similar to Agrawal's approach in which various physical phenomena are assigned different length scales, thus indicating their relative importance [15].

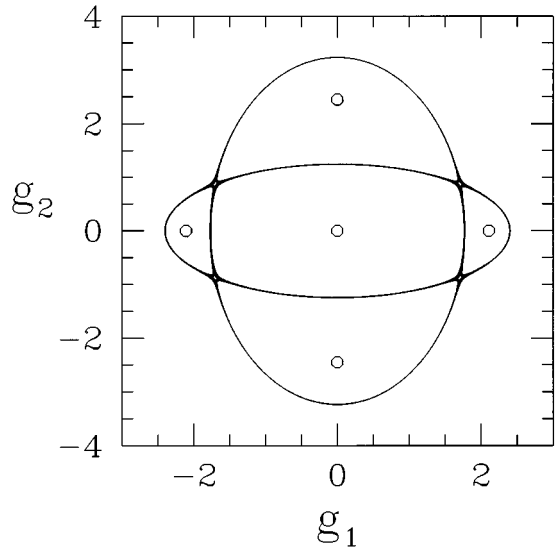

FIG. 12. Separatrices in the (g_1,g_2) plane, corresponding to stationary solutions to the coupled-mode equations. The particular parameters are $\kappa=1$ and $\delta=-5$, while the units of field strength have been chosen such that $\alpha_1=1.0$, $\alpha_2=0.6$ and $\alpha_3=0.9$. Further, $E=-4.06$, where E is the ''energy'' corresponding to the orbit according to Hamiltonian (119). While the saddle points can be clearly seen, the circles correspond to the positions of the centers.

Perhaps our main result is Eq. (102), which is derived for an intensity index $s=1$ (see Sec. IV) and makes use of two Bloch functions from the photonic band structure. It is a generalization of the well-known nonlinear coupled-mode equations for shallow gratings. While even for moderately deep grating structures, such as those consisting of GaAs and AlAs, the conventional coupled-mode equations for shallow structures are remarkably accurate (see Fig. 4), it should be kept in mind that for frequencies around the edges of the photonic band gap the grating properties change drastically. A correct description in this region is thus of particular importance. Nevertheless, it is fair to conclude that deep grating effects are unlikely to be of importance in fiber gratings, where the refractive jump does not exceed 0.04.

An open question at this point is the importance of the remote band effects. As mentioned in the discussion following Eqs. (90), the remote bands, the bands whose Bloch functions enter the analysis only through the companion terms at high orders, lead to an additional (slight) curvature of the bands. At frequencies near the photonic band gap this curvature is negligible compared to the dispersion due to the dynamic interaction of the two bands constituting the principal terms. But further from the gap, the strength of the dynamic interaction drops and remote band effects become more important, though it is not clear how significant they are compared to the intrinsic dispersion of the constituent materials, an effect that has been neglected in our calculations. The latter effect must dominate sufficiently far from Bragg resonances. Initially, the only way to settle this problem is probably on a case-by-case basis.

Possible generalizations of our theory easily come to

mind. Apart from the inclusion of material dispersion, another generalization is to include more than two principal components and thus treat fewer bands as remote. Clearly, the more principal components included, the better the final results, but at the expense of more complicated final results (note that the number of coupled equations in the final result equals the number of principal components). We note that this is a standard procedure in solid state physics, where the number of bands included in $\mathbf{k}\cdot\mathbf{p}$ calculations, for example, to calculate the band structure of superlattices increases with the desired accuracy [22]. However, it follows from our approach that it is not very useful to improve the description of the dispersive properties without a similar effort for the nonlinear properties.

Though we did find different types of solutions to the present coupled-mode equations, such solutions are unlikely to be observed experimentally in the near future due to the high-intensity levels required. The features of low-intensity solutions of the two equations are very similar. This is not surprising because the physical mechanism, Bragg reflection, is, of course, unchanged.

With respect to other applications of our method we note that a coupled-mode-like theory can also be used to describe grating superstructures [30–32]; while for shallow superstructures standard coupled-mode theory can be extended straightforwardly, for deep superstructures this is not sufficient [30]. Although we do not treat grating superstructures here, the method we have developed can also be applied to treat such deep superstructures [31].

In conclusion, we have presented a systematic approach to the derivation of envelope-function equations for nonlinear periodic media. Perhaps unexpectedly, we find that it is possible to derive coupled-mode equations, very much like those that hold for shallow gratings in regimes well beyond where one might naively expect equations of this sort to be valid. Our results reduce to well-known equations in the appropriate limits. We have also presented some of the solutions to these different equations. While they have features that differ qualitatively from those of the solutions to the conventional equations, these occur most clearly at high intensities, which, as yet, are experimentally inaccessible.

ACKNOWLEDGMENTS

This work was supported by the Australian Research Council, by the National Science and Engineering Research Council of Canada, and by the Ontario Laser and Lightwave Research Centre. J.E.S. acknowledges support from the Killam Foundation. The Optical Fibre Technology Centre is a member of the Australian Photonics Cooperative Research Centre.

[1] H.G. Winful, J.H. Marburger, and E. Garmire, Appl. Phys. Lett. **35**, 379 (1979).
[2] W. Chen and D.L. Mills, Phys. Rev. Lett. **58**, 160 (1987).
[3] C.M. de Sterke and J.E. Sipe, Phys. Rev. A **38**, 5149 (1988).
[4] C.M. de Sterke and J.E. Sipe, in *Progress in Optics*, edited by E. Wolf (North-Holland, Amsterdam, 1994), Vol. XXXIII, pp. 203–260.
[5] A.B. Aceves and S. Wabnitz, Phys. Lett. A **141**, 37 (1989).
[6] J. Coste and J. Peyraud, Phys. Rev B **39**, 13 096 (1989).
[7] J. Feng and F. Kneubühl, IEEE J. Quantum Electron. **29**, 590 (1993).
[8] S. Radic, N. George, and G.P. Agrawal, J. Opt. Soc. Am. B **12**, 671 (1995).
[9] N.D. Sankey, D.F. Prelewitz, and T.G. Brown, Appl. Phys. Lett. **60**, 1427 (1992).
[10] M. Cada, J. He, B. Acklin, M. Proctor, D. Martin, F. Morier-Genoud, M.A. Dupertuus, and J.M. Glinsky, Appl. Phys. Lett. **60**, 404 (1992).
[11] C.J. Herbert and M.S. Malcuit, Opt. Lett. **18**, 1783 (1993).
[12] U. Mohideen, R.E. Slusher, V. Mizrahi, T. Erdogan, J.E. Sipe, P.J. Lemaire, C.M. de Sterke, and N.G.R. Broderick, Opt. Lett. **20**, 1674 (1995).
[13] B.J. Eggleton, R.E. Slusher, C.M. de Sterke, P.A. Krug, and J.E. Sipe, Phys. Rev. Lett. **76**, 1627 (1996).
[14] See, e.g., D. Marcuse, *Theory of Dielectric Optical Waveguides*, 2nd ed. (Academic, Boston, 1991), Chap. 3.
[15] G.P. Agrawal, *Nonlinear Fiber Optics* (Academic, San Diego, 1989).
[16] H.A. Macleod, *Thin-Film Optical Filters*, 2nd ed. (Hilger, Birmingham, 1984).
[17] J.E. Sipe, L. Poladian, and C.M. de Sterke, J. Opt. Soc. Am. A **11**, 1307 (1994).
[18] V. Mizrahi, P.J. Lemaire, T. Erdogan, W.A. Reed, D.J. DiGiovanni, and R.M. Atkins, Appl. Phys. Lett. **63**, 1727 (1993).
[19] J. Callaway, *Quantum Theory of the Solid State* (Academic, New York, 1974).
[20] P. St. J. Russell, J. Mod. Opt. **38**, 1599 (1991).
[21] D.G. Salinas, C.M. de Sterke, and J.E. Sipe, Opt. Commun. **111**, 105 (1994).
[22] G. Bastard, J.E. Brum, and R. Ferreira, in *Solid State Physics*, edited by H. Ehrenreich and D. Turnbull (Academic, Vol. 44, Boston, 1991), pp. 229–416.
[23] See, e.g., R.K. Dodd, J.C. Eilbeck, J.D. Gibbons, and H.C. Morris, *Solitons and Nonlinear Wave Equations* (Academic, London, 1982), Ch. 8.
[24] C.M. de Sterke and J.E. Sipe, Phys. Rev. A **39**, 5163 (1989).
[25] C.M. de Sterke, Phys. Rev. E **48**, 4136 (1993).
[26] M. Born and E. Wolf, *Principles of Optics*, 6th ed. (Pergamon, Oxford, 1980), Appendix VIII.
[27] Y.S. Kivshar and N. Flytzanis, Phys. Rev. A **46**, 7972 (1992).
[28] H.G. Winful and G.D. Cooperman, Appl. Phys. Lett. **40**, 298 (1982).
[29] C.M. de Sterke and J.E. Sipe, Phys. Rev. A **42**, 2858 (1990).
[30] C.M. de Sterke and N.G.R. Broderick, Opt. Lett. **20**, 2039 (1995).
[31] N.G.R. Broderick, C.M. de Sterke, and B.J. Eggleton, Phys. Rev. E **52**, R5788 (1995).
[32] B.J. Eggleton, C.M. de Sterke, and R.E. Slusher, Opt. Lett. (to be published).